

1. REPORT NUMBER CA18-3109	2. GOVERNMENT ASSOCIATION NUMBER	3. RECIPIENT'S CATALOG NUMBER
4. TITLE AND SUBTITLE Modeling and Control of HOT lane - Phase II Toolbox development for efficient quantitative assessment of operational scenarios on freeways with managed lanes		5. REPORT DATE 06/03/2019
7. AUTHOR(S) Dr. Alex A Kurzhanskiy, UC Berkeley PATH Program		6. PERFORMING ORGANIZATION CODE
9. PERFORMING ORGANIZATION NAME AND ADDRESS California PATH Program, Institute of Transportation Studies, University of California, Berkeley, Richmond Field Station, 1357 S. 46th Street, Richmond, CA 94804		8. PERFORMING ORGANIZATION REPORT NO.
12. SPONSORING AGENCY AND ADDRESS California Department of Transportation 1727 30th Street, MS-83, Third Floor Sacramento CA 95816		10. WORK UNIT NUMBER
		11. CONTRACT OR GRANT NUMBER 65A0626
		13. TYPE OF REPORT AND PERIOD COVERED Final Report 5/1/17 to 12/31/2018
		14. SPONSORING AGENCY CODE
15. SUPPLEMENTARY NOTES The goal for this project was to develop the toolbox for efficient quantitative assessment of operational scenarios on freeways with managed lanes in terms of vehicle miles traveled (VMT), vehicle hours traveled (VHT), delay, travel time, and toll revenue. This toolbox includes data analysis and modeling components. In addition, work under this project also explored the impact of High Occupancy Toll (HOT) policy violations on the operation of the General Purpose (GP) and the HOT lanes.		
16. ABSTRACT This project extended the driver behavior model with a second, alternative parameterization of HOT violation. To accompany ready-to-pay model, this project developed a concept of a willing-to-violate model. This model describes the portion of non-High Occupancy Vehicle (HOV) drivers that are willing to misrepresent themselves as HOVs to gain free access as a function of several variables, including e.g. the toll cost saved by violation, probability of being caught and the difference of traffic density in the general purpose and the HOT lanes. This parameterization allowed for study of effects on the HOT lane system as a function of estimated probability of catching violators from increased enforcement.		
17. KEY WORDS Quantitative Assessment, High Occupancy Toll (HOT) Policy	18. DISTRIBUTION STATEMENT This document can be distributed with no restriction	
19. SECURITY CLASSIFICATION (of this report) Not a classified document	20. NUMBER OF PAGES 63	21. COST OF REPORT CHARGED

DISCLAIMER STATEMENT

This document is disseminated in the interest of information exchange. The contents of this report reflect the views of the authors who are responsible for the facts and accuracy of the data presented herein. The contents do not necessarily reflect the official views or policies of the State of California or the Federal Highway Administration. This publication does not constitute a standard, specification or regulation. This report does not constitute an endorsement by the Department of any product described herein.

For individuals with sensory disabilities, this document is available in alternate formats. For information, call (916) 654-8899, TTY 711, or write to California Department of Transportation, Division of Research, Innovation and System Information, MS-83, P.O. Box 942873, Sacramento, CA 94273-0001.

Modeling and Control of HOT Lanes - Phase II

Alex A. Kurzhanskiy

June 3, 2019

Contents

- 1 Introduction 7**
 - 1.1 Overview 7
 - 1.2 Problem 8
 - 1.3 Objective 10
 - 1.4 Scope 10

- 2 Methodology 12**
 - 2.1 Multimodal Macroscopic Traffic Model 12
 - 2.2 Modeling HOT Lane 16
 - 2.2.1 Full Access HOT Lane 16
 - 2.2.2 Separated HOT Lane with Control Access 19
 - 2.2.3 HOT Lane Controller 22
 - 2.3 Calibration of HOT Controller 27
 - 2.4 Model Calibration 29
 - 2.4.1 Split Ratios for the Full Access HOT Lane 30

2.4.2	Split Ratios for the Separated HOT Lane	32
2.4.3	Summary of the Calibration Process	34
3	I-10 West: Data Analysis and Simulation	36
3.1	Overview	36
3.2	Violation Data Analysis	41
3.3	Simulation Model	47
3.3.1	Scenario 1	54
3.3.2	Scenario 2	55
3.3.3	Scenario 3	56
4	Conclusion	58

List of Figures

1.1	Speed contours for the GP (left) and the HOT (right) lanes of I-10 West freeway between postmiles 30 and 20 in Los Angeles from Wednesday, August 31, 2016. Source: PeMS [2].	8
2.1	Fundamental diagram.	13
2.2	Freeway with full access HOT lane.	17
2.3	Freeway with separated HOT lane and gates.	20
2.4	A node where some of the input links form travel facilities with some of the output links.	22
2.5	Flow-price curve: toll depends on the total flow entering the HOT link (link 22, as in Figure 2.4). Shown are linear (L), polynomial (P) and sigmoid (S) dependencies.	23
2.6	Value function (left); probability weighting function (right).	25
2.7	A node with a GP link and an on-ramp as inputs, and a GP link and an off-ramp as outputs.	33
2.8	Calibration workflow.	34
3.1	Map of the 12-mile I-10 West freeway segment with the HOT lane	36
3.2	Monthly VMT statistics on I-10 West.	38

3.3	Percentage composition of monthly VMT statistics on I-10 West.	39
3.4	Monthly toll and revenue statistics on I-10 West.	40
3.5	I-10 West HOT lane vehicle counts and counts of type I violations.	41
3.6	I-10 West HOT lane vehicle counts and counts of type I violations during peak hours.	42
3.7	Peak/off-peak breakdown of I-10 West HOT lane type I violation counts.	43
3.8	Comparison of manual counts with FasTrak data at two measurement points.	44
3.9	Ratios of peak hour monthly operations revenue to monthly peak hour VMT and to average toll. Star indicates the time, when manual counts were collected.	45
3.10	Estimated monthly peak hour VMT from violators and revenue loss due to violators.	46
3.11	Map of the 12-mile I-10 West freeway segment with the HOT lane	47
3.12	Estimation of the toll value based on the flow in the HOT lane.	48
3.13	Dependency of rediness to pay on difference of traffic density in the GP and the HOV lanes (left); and on the toll value (right).	49
3.14	Estimation of readiness to pay as a function of density difference between the GP and the HOV lanes and the toll.	50
3.15	Readiness to pay as a function of density difference between the GP and the HOV lanes and the toll.	52
3.16	Readiness to violate as a function of the probability of being caught and the toll.	53
3.17	Scenario 1 — constant LOV and HOV demand.	55
3.18	Scenario 2 — the same as scenario 1, but has higher HOV demand.	56
3.19	Scenario 3 — varying LOV and HOV demand.	57

List of Tables

1.1	Vehicle counts collected on Thursday, September 26, 2013, during peak AM hours, between 7 and 8 AM, on a segment of I-10 West. Source: Caltrans District 7.	9
1.2	List of HOT facilities in California.	11
3.1	2017 satisfaction survey for express lanes on I-10 and I-110 taken by LA Metro. . . .	40
3.2	Toll lookup table.	51
3.3	Varying demand.	56

Acknowledgement

This research was sponsored by the Division of Research, Innovation and System Information (DRISI) of the California Department of Transportation. We would like to specially thank Shahrzad Amiri and Michel'le Davis from LA Metro for providing valuable HOT lane data.

Chapter 1

Introduction

1.1 Overview

This report describes the multimodal *macroscopic* simulation model of freeways with High-Occupancy or Tolloed (HOT) lanes, which captures violators' behavior, and its calibration methodology. It is organized as follows.

- Chapter 2 covers the project methodology.
 - Section 2.1 introduces the underlying multimodal macroscopic traffic model.
 - Section 2.2 shows how this traffic model can be used to capture phenomena of different HOT lane configurations. It provides the details of HOT controller and, particularly, explains how violators' behavior can be modeled.
 - Section 2.3 addresses the calibration of the HOT controller.
 - Section 2.4 discusses the overall model calibration process.
- Chapter 3 analyzes 11-mile segment of I-10 West corridor that has a separated HOT lane with access control.
 - Section 3.1 describes the studied part of the I-10 West corridor providing fundamental statistics of its operation.

- Section 3.2 provides the methodology for assessment of the HOT lane violations and their impact on the HOT lane operation.
- Section 3.3 presents the HOT lane model based on the I-10 West data. Los Angeles County.
- Chapter 4 concludes the report.

1.2 Problem

Available to high-occupancy vehicles without charge, an HOT lane admits other vehicles if they pay a fee, which can be fixed or adjustable based on demand. The idea is that acceptance of more than just high-occupancy vehicles would lead to higher utilization of HOT lanes compared to their HOV counterparts. A dynamic pricing mechanism should control the HOT demand, making it possible to not let the speed in the HOT lane drop below 45 mph. In reality, however, HOT lanes with dynamic pricing often fall below this speed. Figure 1.1 shows the GP and the HOT speed contours for the I-10 West freeway in Los Angeles. As one can see, the HOT lane gets congested during the morning peak hours due to heavy demand.

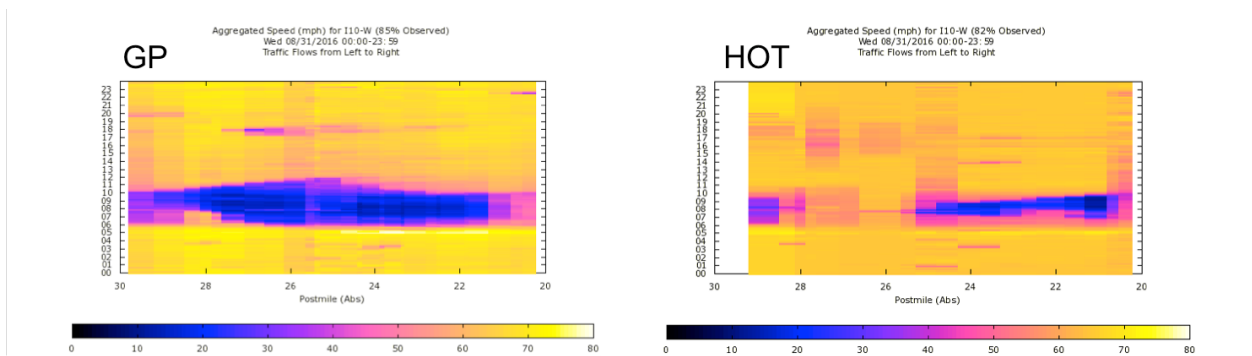


Figure 1.1: Speed contours for the GP (left) and the HOT (right) lanes of I-10 West freeway between postmiles 30 and 20 in Los Angeles from Wednesday, August 31, 2016. Source: PeMS [2].

Here, the GP and HOT lane groups have 4 and 2 lanes, respectively. The HOT lanes are always active, but the toll controller has two regimes corresponding to peak hours — from 5 to 9 am and from 4 to 7 pm on weekdays, and to off-peak hours — the rest of the time. During off-peak hours, HOVs with two passengers or more can use the HOT lane free of charge, and single-occupancy

vehicles (SOVs) can use the HOT lane at the fixed price of 25 cents per mile. During peak hours, HOVs with three passengers or more can use the HOT lane free of charge. The others are considered low-occupancy vehicles (LOVs) and to use the HOT lane have to pay the toll, which varies between 35 and 200 cents per mile depending on the demand for the HOT lane. To use the HOT lane, a vehicle must have a FasTrak transponder, which the driver manually sets to SOV (single-occupancy vehicle), 2+HOV (vehicle with 2 occupants) or 3+HOV (vehicle with 3 or more occupants). The HOT lane facility sets and collects its toll using readings of FasTrak transponders, which are mounted on the vehicles' dashboard by their drivers. At certain points along the HOT lane, FasTrak readers communicate with vehicles' transponders, monitor the amount of vehicle flow, and adjust the toll accordingly. In addition, the HOT lane detectors determine which toll, if any, the driver has to pay, and record the identification numbers of the observed FasTrak transponders, allowing for automatic toll collection by debiting the drivers' FasTrak accounts. In the case depicted in Figure 1.1, the HOT lane gets congested because of the unusually high volume of 3+HOV traffic whose demand is not affected by tolls, and which likely results from LOV drivers evading the toll. Table 1.1 shows a

Vehicle category	FasTrak counts (% of total)	Manual counts (% of total)
SOV	1,567 (52.5%)	2,069 (82.6%)
2+HOV	338 (11.3%)	334 (13.3%)
3+HOV	1,082(36.2%)	101 (4%)
Total	2,987	2,504

Table 1.1: Vehicle counts collected on Thursday, September 26, 2013, during peak AM hours, between 7 and 8 AM, on a segment of I-10 West. Source: Caltrans District 7.

comparison of vehicle counts broken down by vehicle category, SOV, 2+HOV and 3+HOV, for both FasTrak readings and manual counts. Evidently, a large number of 3+HOVs are actually cheating SOVs.

To address this problem, there is a need for methodology and tools for quantitative evaluation of HOT facility operations and assessment of HOT policy violations and their impact.

1.3 Objective

The aim of the current project was to provide a multimodal macroscopic freeway simulation model that captures the phenomena of a HOT lane operation, including the behavior of HOT lane violators, and such that it could be calibrated based on measured vehicle counts and speeds and used for efficient evaluation of operational scenarios on freeways with HOT lanes.

Working toward this goal, we delivered:

1. Theoretical multimodal model of a freeway corridor with a HOT lane;
2. HOT lane control algorithm that accounts for violators' behavior;
3. Implementation of the HOT model and the HOT control algorithm in BeATS;
4. Calibration methodology for the proposed model;
5. HOT lane data analysis and methodology for assessing HOT lane violations and their impact on the HOT lane operation based on the data from I-10 West express lane; and
6. Evaluation of proposed algorithms using I-10 West data.

1.4 Scope

Current list of HOT lane facilities in California is given in Table 1.2, spanning over 330 miles. HOT facilities are becoming popular in the U.S. For example, in the San Francisco Bay Area alone, the Metropolitan Transportation Commission (MTC) promises the implementation of a 550-mile express lane network by 2035, and all of it will be managed with dynamic pricing strategies.

Facility	Description	Carpool occupancy
I-10	11 miles in each direction	3+HOV
I-15	20 miles in each direction	2+HOV
I-110	11 miles in each direction	2+HOV
I-580	14 miles in each direction	2+HOV
I-680 SB Sunol - Milpitas	14 miles	2+HOV
I-680 Contra Costa NB	11 miles	2+HOV
I-680 Contra Costa SB	12 miles	2+HOV
I-880 / SR-237	4 miles in each direction	2+HOV
SR-91	18 miles in each direction	3+HOV
SR-125	22 miles in each direction	2+HOV
I-15 Riverside	14.6 miles in each direction to open in 2020	2+HOV
I-680 SB Martinez - Walnut Creek	11 miles to open in 2020	2+HOV
I-680 NB Milpitas - Sunol	14 miles to open in 2020	2+HOV
I-880 NB Milpitas - Hayward	20 miles to open in 2020	2+HOV
I-880 SB Oakland - Milpitas	25 miles to open in 2020	2+HOV

Table 1.2: List of HOT facilities in California.

Proper deployment and management of HOT facilities relies on the continuous process of:

1. obtaining and analyzing traffic measurement data;
2. operations planning — simulating various scenarios and operational strategies; and
3. implementing the most promising operational strategies in the field.

This process requires a fast and trusted traffic simulator for the rapid quantitative assessment of a large number of operational strategies for the road network under various scenarios. The research presented hereby is an important step for achieving this goal.

Chapter 2

Methodology

2.1 Multimodal Macroscopic Traffic Model

We model traffic flow in a road network consisting of links \mathcal{L} and nodes \mathcal{N} , where links represent stretches of roads, and nodes represent junctions that connect links. A node always has at least one input and at least one output link. A link is called *ordinary* if it has both begin and end nodes. A link with no begin node is called *origin*, and a link with no end node is called *destination*. Origins are links through which vehicles enter the system, and destinations are links that let vehicles out. The traffic state at each moment of time is defined by the number of vehicles of different classes in every link. Different vehicle classes are needed to distinguish between high-occupancy vehicles (HOVs) and low-occupancy vehicles (LOVs) of three categories:

1. willing to pay;
2. willing to violate; and
3. unwilling to use the HOT lane.

Each link $l \in \mathcal{L}$ is characterized by its length and the fundamental diagram, a flow-density relationship presented in Figure 2.1. A fundamental diagram is defined by four values: capacity F_l , free flow speed v_l^f , congestion wave speed w_l and the jam density n_l^J .¹

¹For the sake of notation, in this report we assume these values to be fixed, but in general they may be time-varying.

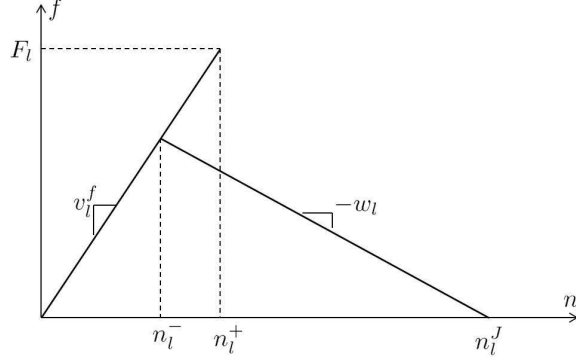


Figure 2.1: Fundamental diagram.

In this report we assume that densities, flows and speeds are *normalized* by link lengths and the discretization time step; ² and that free flow speed v_l^f and congestion wave speed w_l satisfy the Courant-Friedrichs-Lewy (CFL) condition [3]: $0 \leq v_l^f, w_l \leq 1$. ³ The values $n_l^- = \frac{w_l n_l^J}{v_l^f + w_l}$ and $n_l^+ = \frac{F_l}{v_l^f}$ are called *low* and *high critical density* respectively. Unless $n_l^- = n_l^+$, when it assumes triangular shape, the fundamental diagram is not a function of density: $n_l(t) \in (n_l^-, n_l^+]$ admits two possible flow values.

Each node $\nu \in \mathcal{N}$ with M_ν input and N_ν output links is characterized by time dependent mutual restriction intervals $\{\eta_{jj'}^i(t)\}$, input link priorities $\{p_i(t)\}$ and partially defined split ratios $\{\beta_{ij}^c(t)\}$, ⁴ where C is the number of vehicle types; $i = 1, \dots, M_\nu$, $j, j' = 1, \dots, N_\nu$ and $c = 1, \dots, C$.

The state of the system at time t is described by the number of vehicles per commodity in each link: $\vec{n}_l(t) = [n_l^1(t), \dots, n_l^C(t)]^T$, where $n_l^c(t)$ represents the number of vehicles of type c in link l at time t . In our notation, $n_l(t) = \sum_{c=1}^C n_l^c(t)$. The state update equation for link $l \in \mathcal{L}$ is:

$$\vec{n}_l(t+1) = \vec{n}_l(t) + \left(\vec{f}_l^{\text{in}}(t) - \vec{f}_l^{\text{out}}(t) \right), \quad (2.1.1)$$

where $\vec{f}_l^{\text{in}}(t) = [f_l^{1,\text{in}}(t), \dots, f_l^{C,\text{in}}(t)]^T$ is the vector of commodity flows coming into link l during this time step, and $\vec{f}_l^{\text{out}}(t) = [f_l^{1,\text{out}}(t), \dots, f_l^{C,\text{out}}(t)]^T$ is the vector of commodity flows leaving link

²Given original (not normalized) capacity \tilde{F}_l specified in vehicles per hour (vph), free flow speed \tilde{v}_l^f and congestion wave speed \tilde{w}_l specified in miles per hour (mph), and jam density \tilde{n}_l^J specified in vehicles per mile (vpm), as well as link length Δx_l and discretization time step Δt , normalized values are $F_l = \tilde{F}_l \Delta t$ specified in vehicles per time period Δt , $v_l^f = \tilde{v}_l^f \frac{\Delta t}{\Delta x_l}$ and $w_l = \tilde{w}_l \frac{\Delta t}{\Delta x_l}$, both unitless, and $n_l^J = \tilde{n}_l^J \Delta x_l$ specified in vehicles.

³The CFL condition is the necessary condition for convergence while solving hyperbolic PDEs numerically.

⁴Split ratios may also be fully defined or fully undefined.

l during this time step.

For ordinary and destination links, $\vec{f}_l^{in}(t)$ is obtained from the begin node: given a begin node ν with M_ν input links,

$$f_l^{c,in}(t) = \sum_{i=1}^{M_\nu} f_{il}^c(t), \quad c = 1, \dots, C. \quad (2.1.2)$$

For origin links,

$$f_l^{c,in}(t) = d_l^c(t), \quad (2.1.3)$$

where $d_l^c(t)$ denotes commodity demand at time t , which is an exogenous input to the model, specified in vehicles per discretization step Δt .

For ordinary and origin links, $\vec{f}_l^{out}(t)$ is obtained from the end node: given an end node ν with N_ν output links,

$$f_l^{c,out}(t) = \sum_{j=1}^{N_\nu} f_{lj}^c(t), \quad c = 1, \dots, C. \quad (2.1.4)$$

For destination links,

$$f_l^{c,out}(t) = v_l^f n_l^c(t) \min \left\{ 1, \frac{F_l}{\sum_{c'=1}^C v_l^f n_l^{c'}(t)} \right\}, \quad c = 1, \dots, C. \quad (2.1.5)$$

The values $f_{il}^c(t)$ and $f_{lj}^c(t)$ are computed by the node model from [5] (Section 2.1.1).

For each link $l \in \mathcal{L}$ we will also define a congestion metastate:

$$\theta_l(t) = \begin{cases} 0 & n_l(t) \leq n_l^-, \\ 1 & n_l(t) > n_l^+, \\ \theta_l(t-1) & n_l^- < n_l(t) \leq n_l^+. \end{cases} \quad (2.1.6)$$

This metastate helps determining which constraint of the fundamental diagram is activated when we compute the receive function for a link.

Now we can formally describe the LNCTM that runs for T time steps.

1. Initialize:

$$\begin{aligned} n_l^c(0) &:= n_{l,0}^c; \\ \theta_l(0) &:= \theta_{l,0}; \\ t &:= 0 \end{aligned}$$

for all $l \in \mathcal{L}$ and $c = 1, \dots, C$, where $n_{l,0}^c$ and $\theta_{l,0}$ are the initial conditions.

2. Apply all the control functions that modify system parameters (fundamental diagrams, input priorities) and/or system state. A control function may represent ramp metering, variable speed limit, managed lane policy, etc. Control functions may be *open-loop* (if they depend only on time) and *closed-loop* (if they depend on time and system state). This step is optional.
3. For each link $l \in \mathcal{L}$ and commodity $c = 1, \dots, C$ define the *send* function (demand):

$$S_l^c(t) = \begin{cases} v_l^f n_l^c(t) \min \left\{ 1, \frac{F_l}{v_l^f \sum_{c=1}^C n_l^c(t)} \right\}, & l \text{ is an ordinary link or a destination,} \\ d_l^c(t) \min \left\{ 1, \frac{F_l}{\sum_{c=1}^C d_l^c(t)} \right\}, & l \text{ is an origin.} \end{cases} \quad (2.1.7)$$

4. For each link $l \in \mathcal{L}$ define the *receive* function (supply):

$$R_l(t) = \begin{cases} (1 - \theta_l(t)) F_l + \theta_l(t) w_l \left(n_l^J - \sum_{c=1}^C n_l^c(t) \right), & l \text{ is an ordinary link or a destination,} \\ \infty, & l \text{ is an origin.} \end{cases} \quad (2.1.8)$$

5. For each node $\nu \in \mathcal{N}$ with input links $\{i\}$ and output links $\{j\}$ that has undefined split ratios, given its input link priorities $\{p_i(t)\}$, send functions $S_i^c(t)$ and receive functions $R_j(t)$, compute the undefined split ratios $\{\beta_{ij}^c(t)\}$ according to the algorithm from [5] (Section 2.1.2).
6. For each node $\nu \in \mathcal{N}$ with input links $\{i\}$ and output links $\{j\}$, given its mutual restriction intervals $\{\eta_{jj}^i(t)\}$, input link priorities $\{p_i(t)\}$ and split ratios $\{\beta_{ij}^c(t)\}$, send functions $S_i^c(t)$

and receive functions $R_j(t)$, compute input-output flows $f_{ij}^c(t)$ according to the algorithm from [5] (Section 2.1.1).

7. For each link $l \in \mathcal{L}$, compute $\vec{f}_l^{in}(t)$ using expressions (2.1.2)-(2.1.3) and $\vec{f}_l^{out}(t)$ using expressions (2.1.4)-(2.1.5).
8. For each link $l \in \mathcal{L}$, update the state $\vec{n}_l(t+1)$ according to the conservation equation (2.1.1), and the metastate $\theta_l(t+1)$ according to its definition (2.1.6).
9. If $t = T$, then stop, otherwise set $t := t + 1$ and return to step 2.

Traffic speed for link l is computed as a ratio of total flow leaving this link to the total number of vehicles in this link:

$$v_l(t) = \begin{cases} \frac{\sum_{c=1}^C f_l^{c,out}(t)}{\sum_{c=1}^C n_l^c(t)}, & \text{if } \sum_{c=1}^C n_l^c(t) > 0, \\ v_l^f, & \text{otherwise.} \end{cases} \quad (2.1.9)$$

Defined this way, $v_l(t) \in [0, v_l^f]$.

2.2 Modeling HOT Lane

We will consider two types of HOT configurations: *full access* and *separated with control access*. Full access is the configuration where the HOT lane is just another freeway lane, to (from) which eligible vehicles may switch from (to) the general purpose (GP) lane anywhere. A separated HOT lane allows traffic from and to the GP lane only at certain locations, called *gates*. Both, full access and separated HOT lanes may have periods when they act as GP lanes: everybody can use them for free.

2.2.1 Full Access HOT Lane

A full access HOT lane configuration is presented in Figure 2.2: GP and HOT links are parallel with the same geometry and share the same begin and end node pairs; traffic flow exchange between GP

and HOT lanes can happen at every node. Links that are too long may be broken up into smaller ones by creating more nodes, such as nodes 2 and 3 in Figure 2.2. Generally, fundamental diagrams for parallel GP and HOT links are different.

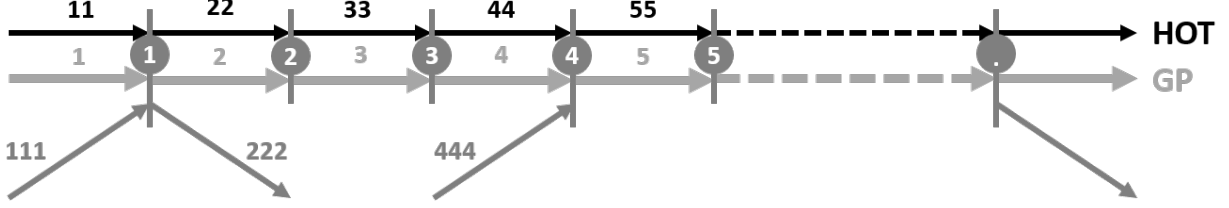


Figure 2.2: Freeway with full access HOT lane.

We introduce four traffic commodities ($C = 4$): $c = 1$ corresponds to the low occupancy vehicle (LOV) traffic not willing to use the HOT lane; $c = 2$ corresponds to the HOV traffic; $c = 3$ corresponds to the LOV traffic ready to pay; and $c = 4$ corresponds to the LOV traffic not ready to pay, but ready to violate. We will refer to $c = 3$ -traffic as *ready to pay*, and to $c = 4$ -traffic as *potential violators*. When HOT lane is active, $c = 1$ -traffic is confined to the GP lane, whereas $c = \{2, 3, 4\}$ -traffic can use both GP and HOT lanes. E.g., for node 1 in Figure 2.2 this policy translates to:

$$\begin{aligned}
 \beta_{1,2}^1 &= 1 - \beta_{1,222}^1 & \beta_{1,22}^1 &= 0 & \beta_{1,222}^1 & \\
 \beta_{11,2}^1 &= 1 - \beta_{11,222}^1 & \beta_{11,22}^1 &= 0 & \beta_{11,222}^1 & \\
 \beta_{111,2}^1 &= 1 - \beta_{111,222}^1 & \beta_{111,22}^1 &= 0 & \beta_{111,222}^1 & \\
 \beta_{1,2}^c &= ? & \beta_{1,22}^c &= ? & \beta_{1,222}^c & \quad \bar{\beta}_1^c = 1 - \beta_{1,222}^c; \\
 \beta_{11,2}^c &= ? & \beta_{11,22}^c &= ? & \beta_{11,222}^c & \quad \bar{\beta}_{11}^c = 1 - \beta_{11,222}^c; \\
 \beta_{111,2}^c &= ? & \beta_{111,22}^c &= ? & \beta_{111,222}^c & \quad \bar{\beta}_{111}^c = 1 - \beta_{111,222}^c,
 \end{aligned} \tag{2.2.1}$$

where $c = 2, 3, 4$; $\beta_{i,222}^1$ $\beta_{i,222}^c$, are given (for example, computed from off-ramp detector measurements), and $\beta_{i,j}^2$ are to be determined using the split ratio assignment algorithm from [5] (Section

2.1.2), $i = 1, 11, 111$, $j = 2, 22$. Similarly, for node 2:

$$\begin{aligned}
\beta_{2,3}^1 &= 1 & \beta_{2,33}^1 &= 0; \\
\beta_{22,3}^1 &= 1 & \beta_{22,33}^1 &= 0; \\
\beta_{2,3}^c &= ? & \beta_{2,33}^c &= ? & \bar{\beta}_2^c &= 1; \\
\beta_{22,3}^c &= ? & \beta_{22,33}^c &= ? & \bar{\beta}_{22}^c &= 1.
\end{aligned} \tag{2.2.2}$$

When the HOT lane becomes available for all traffic free of charge, split ratios for GP and HOT output links are to be determined for both vehicle types. So, for node 1 we have:

$$\begin{aligned}
\beta_{i,j}^c &= ? & \beta_{i,222}^c & & \bar{\beta}_i^c &= 1 - \beta_{i,222}^c; \\
i &= 1, 11, 111; & j &= 2, 22; & c &= 1, 2, 3, 4;
\end{aligned} \tag{2.2.3}$$

and for node 2:

$$\begin{aligned}
\beta_{i,j}^c &= ? & \bar{\beta}_i^c &= 1; \\
i &= 2, 22; & j &= 3, 33; & c &= 1, 2, 3, 4.
\end{aligned} \tag{2.2.4}$$

Note that in this case traffic for classes $c = 3, 4$ will be zero, which does not prevent us from computing the corresponding split ratios.

In this report we do not insist on any particular way of setting link priorities. One common-sense approach inspired by Tampère et al. [10] would be to make priorities proportional to link capacities, which for node 1 in Figure 2.2, will produce:

$$p_i = \frac{F_i}{F_1 + F_{11} + F_{111}}, \quad i = 1, 11, 111.$$

In some cases it makes sense to assign higher priorities to on-ramps. For example, if link 5 in Figure 2.2 has an auxiliary lane starting from node 4, which allows all (or almost all) traffic to enter freeway from on-ramp 444 even when link 5 is congested. In this situation we would set priority p_{444} proportional to $2F_{444}$. Thus, it is reasonable to set priorities of GP and HOT links proportional to their capacities, whereas on-ramp priorities depend on the configuration of the on-ramp and the freeway merging section.

Other parameters that largely depend on the freeway configuration are the mutual restriction intervals. Denote the number of sublanes⁵ in links 1, 2 and 22 of Figure 2.2 L_1 , L_2 and L_{22} respectively, and let $L_{1,222} < L_1$ be the number of sublanes in link 1, from which traffic can exit to the off-ramp 222. Then, one possible way of setting mutual restriction intervals would be:

$$\begin{aligned}
\boldsymbol{\eta}_{2,2}^i &= [0, 1] & \boldsymbol{\eta}_{2,22}^i &= \left[1 - \frac{1}{L_{22}}, 1\right] & \boldsymbol{\eta}_{2,222}^i &= [0, 1]; \\
\boldsymbol{\eta}_{22,2}^i &= \left[0, \frac{1}{L_2}\right] & \boldsymbol{\eta}_{22,22}^i &= [0, 1] & \boldsymbol{\eta}_{22,222}^i &= [0, 0]; \\
\boldsymbol{\eta}_{222,2}^i &= \left[1 - \frac{L_{1,222}}{L_1}, 1\right] & \boldsymbol{\eta}_{222,22}^i &= [0, 0] & \boldsymbol{\eta}_{222,222}^i &= [0, 1],
\end{aligned} \tag{2.2.5}$$

for all input links of node 1: $i = 1, 11, 111$. With such mutual restriction intervals we suggest that shortage of supply in GP link 2 affects the whole flow to the off-ramp 222 ($\boldsymbol{\eta}_{2,222}^i = [0, 1]$) and affects flow in one of the lanes of HOT link 22 ($\boldsymbol{\eta}_{2,22}^i = \left[1 - \frac{1}{L_{22}}, 1\right]$); shortage of supply in HOT link 22 affects flow in one of the lanes of GP link 2 ($\boldsymbol{\eta}_{22,2}^i = \left[0, \frac{1}{L_2}\right]$) and does not affect the off-ramp flow ($\boldsymbol{\eta}_{22,222}^i = [0, 0]$); shortage of supply in the off-ramp 222 affects flow in GP link 2 proportionally to the ratio of the number of lanes that send traffic to the off-ramp in link 1 to the total number of lanes in that link ($\boldsymbol{\eta}_{222,2}^i = \left[1 - \frac{L_{1,222}}{L_1}, 1\right]$) and does not affect the flow in HOT link 22 ($\boldsymbol{\eta}_{222,22}^i = [0, 0]$). A conservative alternative to this approach would be to set all mutual restriction intervals to 1, thus fully enforcing the FIFO rule.

2.2.2 Separated HOT Lane with Control Access

The configuration of the separated HOT lane with control access is presented in Figure 2.3: GP and HOT lanes are treated as two separate freeways that have some common nodes that allow flow exchange between these two freeways. These nodes are *gates*. In the freeway with a full access HOT lane discussed previously, every node is a gate. We can disable flow exchange at a given node by fixing split ratios so that they keep traffic in its lane. For example, to disable the gate (the flow exchange between the two lanes) at node 2 in Figure 2.2, we set $\beta_{2,3}^c = 1$ and $\beta_{22,33}^c = 1$ ($\beta_{2,33}^c = 0$ and $\beta_{22,3}^c = 0$), $c = 1, 2, 3, 4$. Thus, the full access HOT lane can be easily converted into the separated HOT lane by fixing split ratios everywhere but designated gate-nodes. In practice, a gate

⁵We use the term ‘‘sublane’’ here to avoid confusion with the term ‘‘lane’’, which throughout this report is synonymous to ‘‘facility’’. So, when we say that an HOT lane has 2 sublanes and a GP lane has 4 sublanes, we actually mean that the freeway has 2 HOT and 4 GP lanes.

is stretch of freeway about 0.5 miles long, and, potentially, we can designate two or three nodes in a row as gates. However, we assume that a gate is a single node.

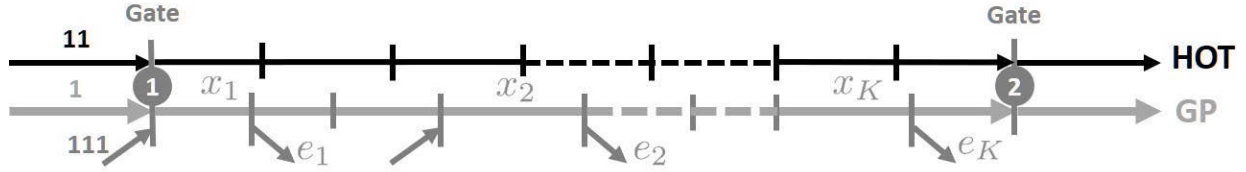


Figure 2.3: Freeway with separated HOT lane and gates.

For the separated HOT configuration, we suggest setting mutual restriction coefficients just as in the case of full access HOT lane, according to formula (2.2.5).

Directing Traffic from the HOT Lane to Off-Ramps

In the full access HOT model, we could direct traffic from the HOT lane to off-ramps by setting corresponding split ratios, e.g. $\beta_{11,222}^c$, $c = 1, 2$, for node 1 in configuration from Figure 2.2. The challenge of the separated HOT lane modeling is that generally gates do not coincide with off-ramp locations. Typically, there are between 2 and 5 off-ramps in the freeway segment from one gate to the next. Off-ramps in the GP road segment connecting two gates in Figure 2.3 are identified as exits e_1, e_2, \dots, e_K , and they cannot be accessed directly from the HOT lane. Vehicles traveling in the HOT lane that intend to take one of the exits e_1, \dots, e_K , must switch from the HOT lane to the GP lane at gate-node 1 and then be directed to the correct off-ramp.

To resolve this challenge, we introduce new traffic commodities in addition to already existing $c = 1$ (LOVs), $c = 2$ (HOVs), $c = 3$ (ready to pay) and $c = 4$ (potential violators) that were introduced in the full access HOT lane model, Section 2.2.1. These additional commodities will be used to distinguish traffic by its destination off-ramp. Assuming that K is the largest number of off-ramps in the GP lane between two adjacent gates, altogether we have $C = K + 4$ traffic commodities: $c = 1, 2, e_1, \dots, e_K$, where e_k indicates the destination

off-ramp in reference to Figure 2.3. By definition, traffic of type $c = e_k$ may exist in the GP lane segment between gate 1 and off-ramp e_k , but there is *no traffic of this type* either in the GP lane segment between off-ramp e_k and gate 2 or in the HOV lane. To ensure this, we set *constant* split

ratios:

$$\begin{aligned}
\beta_{i,x_1}^{e_k} &= 1, \quad i = 1, 11, 111, && \text{direct all } e_k\text{-type traffic to the GP lane at gate 1;} \\
\beta_{x_k, e_k}^{e_k} &= 1, && \text{direct all } e_k\text{-type traffic to off-ramp } e_k; \\
\beta_{x_{k'}, e_{k'}}^{e_k} &= 0, \quad k' \neq k, && \text{do not send any } e_k\text{-type traffic to other off-ramps,}
\end{aligned} \tag{2.2.6}$$

where $k = 1, \dots, K$, and x_k denotes the input GP link for the node that has the output link e_k (see Figure 2.3).

Now we explain how e_k -type traffic appears in the system. The original demand $d_l^c(\cdot)$ is specified at origin links l for commodities $c = 1, 2, 3, 4$, and $d_l^{e_k}(\cdot) \equiv 0$, $k = 1, \dots, K$. Destination specific traffic appears in the HOT links that end at gate-nodes by assigning destinations to portions of the type-1 (LOV), type-2 (HOV) type-3 (ready to pay) and type-4 (potential violators) traffic in those links. We propose incorporating this destination assignment into the step 2 of the traffic model, applying control (Section 2.1) and using off-ramp split ratios β_{x_k, e_k}^c , $c = 1, 2$, $k = 1, \dots, K$, to determine portions of HOT lane traffic to be assigned particular destinations. The destination assignment algorithm at a given time t , for a given HOT link ending with a gate-node, is described next. Without the loss of generality, we will refer to Figure 2.3 and the HOT link 11 ending at the gate-node 1 in this description.

1. Given are vehicle counts per commodity n_{11}^c , $c = 1, 2, e_1, \dots, e_K$; free flow speed v_{11} ; and off-ramp split ratios β_{x_k, e_k}^1 and β_{x_k, e_k}^2 , $k = 1, \dots, K$.⁶

2. Initialize:

$$\begin{aligned}
\tilde{n}_{11}^c(0) &:= n_{11}^c, \quad c = 1, 2, e_1, \dots, e_K; \\
k &:= 1.
\end{aligned}$$

⁶If a given GP segment connecting two adjacent gates has K' off-ramps, where $K' < K$, then assume $\beta_{x_k, e_k}^1 = \beta_{x_k, e_k}^2 = 0$ for $k \in (K', K]$.

3. Assign e_k -type traffic:

$$\tilde{n}_{11}^{e_k}(k) = \tilde{n}_{11}^{e_k}(k-1) + \beta_{x_k, e_k}^1 v_{11} \tilde{n}_{11}^1(k-1) + \beta_{x_k, e_k}^2 v_{11} \tilde{n}_{11}^2(k-1); \quad (2.2.7)$$

$$\tilde{n}_{11}^1(k) = \tilde{n}_{11}^1(k-1) - \beta_{x_k, e_k}^1 v_{11} \tilde{n}_{11}^1(k-1); \quad (2.2.8)$$

$$\tilde{n}_{11}^2(k) = \tilde{n}_{11}^2(k-1) - \beta_{x_k, e_k}^2 v_{11} \tilde{n}_{11}^2(k-1). \quad (2.2.9)$$

4. If $k < K$, then set $k := k + 1$ and return to step 3.

5. Update the state:

$$n_{11}^c = \tilde{n}_{11}^c(K), \quad c = 1, 2, e_1, \dots, e_K.$$

2.2.3 HOT Lane Controller

The other component of the HOT model is the HOT controller consisting of three parts:

1. Calculation of the toll based on the vehicle flow in the HOT lane; and
2. Calculation of the portion of LOVs ready to pay given toll and reassigning vehicles from class $c = 1$ to $c = 3$ accordingly.
3. Calculation of the portion of LOVs ready to violate and reassigning vehicles from what remains in class $c = 1$ to $c = 4$ accordingly.

We shall refer to Figure 2.4 to explain the concept.

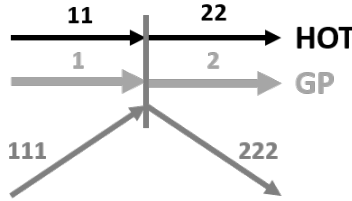


Figure 2.4: A node where some of the input links form travel facilities with some of the output links.

Toll $\pi(\cdot)$ varies between its minimal and maximal values, π_{\min} and π_{\max} , and is computed from the *flow-price curve*, depicted in Figure 2.5, where f_{22}^{in} denotes total flow entering link 22 in Figure 2.4. The flow-price curve is defined by the HOT lane operator in the form of lookup table.

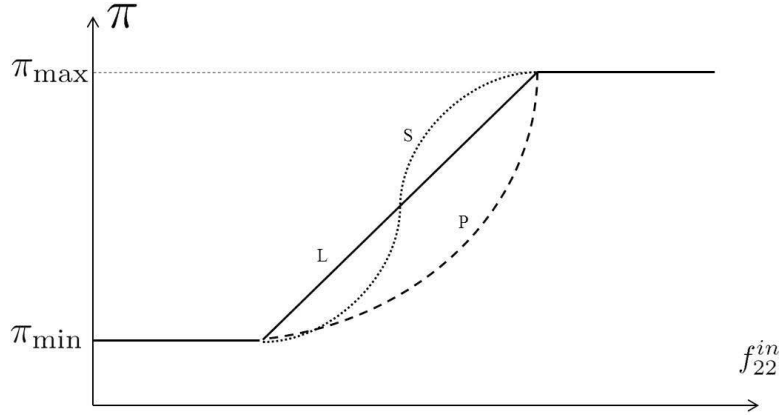


Figure 2.5: Flow-price curve: toll depends on the total flow entering the HOT link (link 22, as in Figure 2.4). Shown are linear (L), polynomial (P) and sigmoid (S) dependencies.

In the second part of the HOT controller we should determine the portion of LOVs ready to pay given price for using HOT lane. The readiness to pay may depend on multiple factors, most obvious of which are:

1. Toll value;
2. Difference in traffic density between GP and HOT lanes;
3. The estimated gain in travel time of the HOT lane over the GP lane; and
4. Travel time reliability.

In this project, we considered readiness to pay depending on items 1 and 2 — toll value and the difference between the GP and the HOT traffic densities.⁷

Using the link numeration from Figure 2.4, the portion $\rho(t)$ of LOVs ready to pay toll $\pi(f_{22}^{in}(t))$ in

⁷We did not include travel time and travel time reliability, because the analysis of I-10 East and West HOT lane data showed that there are always paying LOVs in the HOT lane, even during time periods when GP lane is *always* in free flow.

link 1 at time t is:

$$\rho(t) = \frac{1}{1 + e^{-z(t)}}, \quad \text{where } z(t) = \alpha_0 + \alpha_1 \sum_{c=1}^C \left(\frac{n_2^c(t)}{L_2} - \frac{n_{22}^c(t)}{L_{22}} \right) + \alpha_2 \pi (f_{22}^{in}(t)). \quad (2.2.10)$$

Here, $n_2^c(t)$, $n_{22}^c(t)$ are the vehicle counts in links 2 and 22 from Figure 2.4, respectively; L_2 , L_{22} are lane counts in those links; and $\alpha_0, \alpha_1, \alpha_2$ are known coefficients determined through calibration of the HOT controller (see Section 2.3).

Given the vehicle counts per commodity $n_1^c(t)$ and $n_{111}^c(t)$, $c = 1 \dots, C$, and the portion of LOVs ready to pay $\rho(t)$, the HOT controller adjusts commodity counts as follows:

$$\tilde{n}_1^1(t) = (1 - \rho(t)) \left(\sum_{c \neq 2} n_1^c(t) \right), \quad \tilde{n}_1^3(t) = \rho(t) \left(\sum_{c \neq 2} n_1^c(t) \right), \quad \tilde{n}_1^4(t) = 0; \quad (2.2.11)$$

$$\tilde{n}_{111}^1(t) = (1 - \rho(t)) \left(\sum_{c \neq 2} n_{111}^c(t) \right), \quad \tilde{n}_{111}^3(t) = \rho(t) \left(\sum_{c \neq 2} n_{111}^c(t) \right), \quad \tilde{n}_{111}^4(t) = 0. \quad (2.2.12)$$

Here, the link IDs refer to the configuration in Figure 2.4. We do not adjust commodities in the HOT link 11, because only ready to pay LOVs may be there.⁸

The third part of the HOT controller computes the portion of the remaining LOVs that is ready to violate:

$$\tilde{\rho}(t) = \frac{1}{1 + e^{-\tilde{z}(t)}}, \quad (2.2.13)$$

whose form is similar to that of expression (2.2.10), and the difference is in function $\tilde{z}(t)$. To compute $\tilde{z}(t)$, we invoke the *prospect theory* [7]. This is a theory in cognitive psychology that describes the way people choose between probabilistic alternatives that involve risk, where the probabilities of outcomes are uncertain. The theory states that people make decisions based on the potential value of losses and gains rather than the final outcome, and that people evaluate these losses and gains

⁸Existing HOT policies are such that once a vehicle enters the HOT lane, its toll is set, and it is guaranteed that the driver would not be charged more than that. Thus, we can assume that those LOVs that were ready to pay and ended up in the HOT lane will stay ready to pay.

using some heuristics. It describes the decision process in two stages: (1) editing; and (2) evaluation. During the initial phase termed editing, outcomes of a decision are ordered according to a certain heuristic. In particular, people decide which outcomes they consider equivalent, set a reference point and then consider lesser outcomes as losses and greater ones as gains.

In our model, for an HOT violators there may be two outcomes: x_1 — gain in the amount of a toll value, if they are not caught; and x_2 — loss in the amount of a fine⁹.

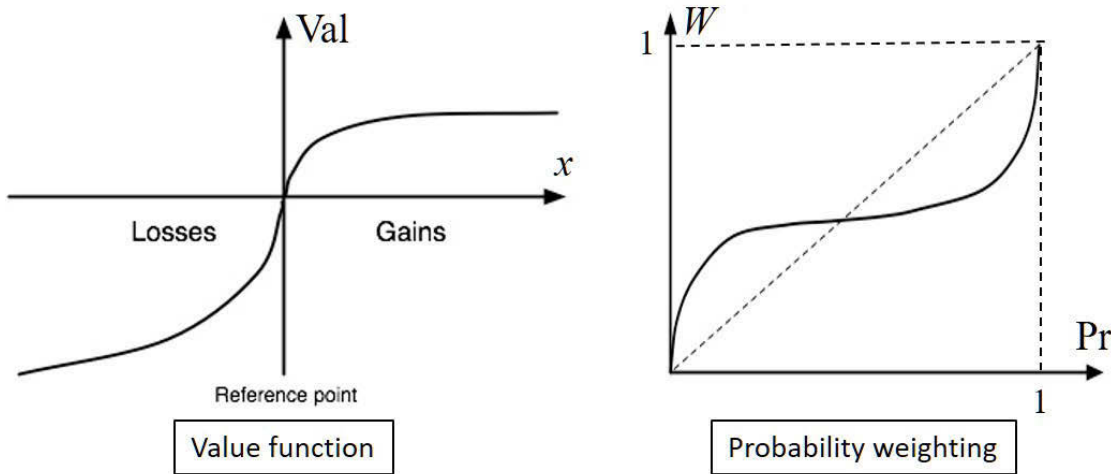


Figure 2.6: Value function (left); probability weighting function (right).

these outcomes have probabilities Pr_1 and $\text{Pr}_2 = 1 - \text{Pr}_1$ respectively.

In the subsequent evaluation phase, people behave as if they would compute a value (utility), based on the potential outcomes and their respective probabilities, and then choose the alternative having a higher value. Each outcome has a value for potential violators: $\text{Val}(x_1)$ and $\text{Val}(x_2)$. Presented in Figure 2.6 (left), the value function that passes through the reference point is s-shaped and asymmetrical. Losses hurt more than gains feel good (loss aversion). This differs from expected utility theory [9], in which a rational agent is indifferent to the reference point. In the expected utility theory, the individual does not care how the outcome of losses and gains are framed.

The probabilities of outcomes in the prospect theory are assessed using the *weighting function* $W(\text{Pr})$, presented in Figure 2.6 (right), which captures the idea that people tend to overreact to

⁹Presently, the minimal fine for HOT violation is \$ 490. This is for the first-time violators. Those caught more than one time have to pay a larger price.

small probability events, but underreact to large probabilities.

The recommended form of the value function is [11]:

$$\text{Val}(x) = \begin{cases} x^\gamma, & x \geq 0; \\ -\lambda(-x)^\gamma, & x < 0. \end{cases} \quad (2.2.14)$$

where λ is some positive parameter and parameter $\gamma \in (0, 1)$.

The recommended form of the probability weighting function is [11]:

$$W(\text{Pr}) = \frac{\text{Pr}^\alpha}{(\text{Pr}^\alpha + (1 - \text{Pr})^\alpha)^{1/\alpha}}, \quad (2.2.15)$$

where parameter $\alpha \in (0, 1)$.

Thus, the evaluation phase of the third part of the HOT controller can be expressed as:

$$\tilde{z}(t) = \kappa (W(\text{Pr}_1)\text{Val}(x_1(t)) + W(1 - \text{Pr}_1)\text{Val}(x_2)), \quad (2.2.16)$$

where κ is some nonnegative constant, gain $x_1(t) = \pi (f_{22}^{in}(t)) \text{Dist}$ (here Dist represents the remaining travel distance), loss x_2 is the fine one would have to pay if caught, Pr_1 is the probability that a violator will not be caught, $\text{Val}(x)$ is the value function defined in (2.2.14) and $W(\text{Pr})$ is the weighting function defined in (2.2.15). Formula (2.2.16) completes the expression (2.2.13).

Given the adjusted vehicle counts per commodity $\tilde{n}_1^c(t)$ and $\tilde{n}_{111}^c(t)$, $c = 1 \dots, C$, and the portion of LOVs ready to violate $\tilde{\rho}(t)$, the HOT controller adjusts commodity counts as follows:

$$\tilde{n}_1^1(t) = (1 - \tilde{\rho}(t))\tilde{n}_1^1(t), \quad \tilde{n}_1^3(t) = \tilde{n}_1^3(t), \quad \tilde{n}_1^4(t) = \tilde{\rho}(t)\tilde{n}_1^1(t); \quad (2.2.17)$$

$$\tilde{n}_{111}^1(t) = (1 - \tilde{\rho}(t))\tilde{n}_{111}^1(t), \quad \tilde{n}_{111}^3(t) = \tilde{n}_{111}^3(t), \quad \tilde{n}_{111}^4(t) = \tilde{\rho}(t)\tilde{n}_{111}^1(t). \quad (2.2.18)$$

Now we can summarize the action of the HOT controller:

1. Determine toll π from the flow-price curve in Figure 2.5.
2. Compute $\rho(t)$ using formula (2.2.10).
3. Adjust commodity counts using formulae (2.2.11)-(2.2.12).
4. Adjust commodity counts again using formulae (2.2.17)-(2.2.18).

Note that steps 2 and 3 of the controller can be swapped. It can be achieved by replacing $\rho(t)$ with $\tilde{\rho}(t)$ in formulae (2.2.11)-(2.2.12) and vice versa — replacing $\tilde{\rho}(t)$ with $\rho(t)$ in formulae (2.2.17)-(2.2.18).

The HOT controller works on all GP links and on-ramps whose end node is a gate (in full access configuration, every node is a gate). This controller is activated in the step 2 of the traffic model (see Section 2.1). Not all ready to pay or violate vehicles end up in the HOT lane, but only those assigned to it in step 5 (split ratio assignment) of the traffic model. The HOT controller step, that computes the violator's portion $\tilde{\rho}(t)$, works independently of the step determining ready to pay portion of traffic, but both of these steps depend on the computed toll value. In the freeways with no physical barrier between the GP and the HOT lanes, this HOT controller step may be invoked at all nodes (not just gates). That enables the violators to cross over to the HOT lane anywhere.

2.3 Calibration of HOT Controller

To compute coefficients $\alpha_0, \alpha_1, \alpha_2$ for the formula (2.2.10), we make the following assumptions:

1. We can count vehicles in the GP lane, \hat{n}_{GP}^t , and in the HOT lane, \hat{n}_{HOT}^t at any given time t .
2. We have data to estimate the LOV traffic portion ready to pay at time t , $\hat{\rho}^t$:

$$\hat{\rho}^t = \frac{\text{Number of LOVs in the HOT link at time } t}{\text{Total number of LOVs in both HOT and GP links at time } t}. \quad (2.3.1)$$

The nominator in the right hand side of this formula comes from FasTrak data collected in the HOT lane — if the vehicle pays, it is LOV, otherwise it is HOV. The denominator in the right

hand side of this formula is computed as a sum of vehicle count in the GP lane, which can be obtained from PeMS [2], and the number of LOVs in the HOT lane. Obviously, $\hat{\rho} \in [0, 1]$.

3. We know HOT price per mile at time t , π^t , which comes from the FasTrak toll logs.
4. If traffic density per lane in the GP and the HOT lanes were the same and no tolls were collected, we assume the readiness to pay $\rho = \frac{L_{HOT}}{L_{GP} + L_{HOT}}$, where L_{GP} and L_{HOT} denote lane counts in GP and HOT links (links 2 and 22 from Figure 2.4 respectively). According to (2.2.10),

$$\rho = \frac{1}{1 + e^{-\alpha_0}} = \frac{e^{\alpha_0}}{1 + e^{\alpha_0}} = \frac{L_{HOT}}{L_{GP} + L_{HOT}}. \quad (2.3.2)$$

Hence,

$$\alpha_0 = \ln \left(\frac{\rho}{1 - \rho} \right) = \ln \left(\frac{L_{HOT}}{L_{GP}} \right). \quad (2.3.3)$$

Thus, it remains to determine coefficients α_1 and α_2 .

We will estimate α_1, α_2 from equations:

$$\ln \left(\frac{\hat{\rho}^t}{1 - \hat{\rho}^t} \right) = \ln \left(\frac{L_{HOT}}{L_{GP}} \right) + \alpha_1 \left(\frac{\hat{n}_{GP}^t}{L_{GP}} - \frac{\hat{n}_{HOT}^t}{L_{HOT}} \right) + \alpha_2 \pi^t, \quad t = 1, \dots, \Theta. \quad (2.3.4)$$

Denote:

$$\mathbf{X} = \begin{pmatrix} \frac{\hat{n}_{GP}^1}{L_{GP}} - \frac{\hat{n}_{HOT}^1}{L_{HOT}} & \pi^1 \\ \dots & \dots \\ \frac{\hat{n}_{GP}^\Theta}{L_{GP}} - \frac{\hat{n}_{HOT}^\Theta}{L_{HOT}} & \pi^\Theta \end{pmatrix}, \quad \text{and} \quad \mathbf{Y} = \begin{pmatrix} \ln \left(\frac{\hat{\rho}^1}{1 - \hat{\rho}^1} \right) - \ln \left(\frac{L_{HOT}}{L_{GP}} \right) \\ \vdots \\ \ln \left(\frac{\hat{\rho}^\Theta}{1 - \hat{\rho}^\Theta} \right) - \ln \left(\frac{L_{HOT}}{L_{GP}} \right) \end{pmatrix}. \quad (2.3.5)$$

Equations (2.3.4) can be rewritten as:

$$\mathbf{Y} = \mathbf{X} \begin{pmatrix} \alpha_1 \\ \alpha_2 \end{pmatrix}. \quad (2.3.6)$$

Thus, α_1, α_2 can be estimated using the least squares method:

$$\begin{pmatrix} \alpha_1 \\ \alpha_2 \end{pmatrix} = (\mathbf{X}^T \mathbf{X})^{-1} \mathbf{X}^T \mathbf{Y}. \quad (2.3.7)$$

For the HOT controller part that computes the portion of LOVs ready to violate, we need:

- Parameters λ and γ for the value function (2.2.14). We will use the recommended values $\lambda = 1.5$ and $\gamma = 0.88$ [11].
- Parameter α for the probability weighting function (2.2.15). We will use the recommended value $\alpha = 0.6$ [11].
- Probability of a successful violation (not being caught), Pr_1 . Generally, this parameter is computed as a function of system state as the model evolves in time:

$$\text{Pr}_1(t) = 1 - \text{Pr}_2(t) = 1 - \frac{\text{Number of Violating LOVs in HOT Link}(t)}{\text{Total Number of LOVs in HOT Link}(t)} \quad (2.3.8)$$

We suggest setting the initial value for this probability as:

$$\text{Pr}_1 = 1 - \text{Pr}_2 = 1 - \frac{\text{Average number of daily CHP citations for HOT violation}}{\text{Average number of daily peak 5-minute slots}}. \quad (2.3.9)$$

- We choose parameter $\kappa = 0.01$.

2.4 Model Calibration

When it comes to the simulation of real world traffic networks, in our case freeways with HOT lanes, the quality of the simulation results is assessed by comparing them with detector measurements. We expect to have flow and speed measurements at the freeway mainline (from both GP and HOT lanes), as well as flow measurements at on- and off-ramps. To better match the detector measurements the simulation model needs to be tuned. Tunable parameters of our model are:

- Fundamental diagram parameters, free flow speed v_l , congestion wave speed w_l , capacity F_l and the jam density n_l^J , for each link. Calibration of the fundamental diagram is typically model-agnostic, and there exists an abundant research on this topic, including from some of the authors of this report, e.g. [4]. So, we shall assume that this problem is solved.
- Percentage of high-occupancy vehicles in the traffic flow entering the system. This parameter depends on the time of day and location as well as on the type of HOT lane.¹⁰ It could be roughly estimated as a ratio of the HOT lane vehicle count to the total freeway vehicle count during periods of congestion at any given location.
- Inertia coefficients. See [5] (the second part of Section 2.1.2).
- Friction coefficients. See [5] (the second part of Section 2.2.1). In [6] the dependency of the HOV lane speed on the GP lane speed was investigated under different occupancy of the HOV lane, and the presented data suggests that although the correlation between the two speeds exists, it is not very strong, below 0.4. Therefore, we suggest setting friction coefficients to values not exceeding 0.4.
- Mutual restriction intervals. It is also an open question how to estimate mutual restriction intervals from the measurement data. We suggest using expression (2.2.5) as a default guideline.
- Off-ramp split ratios. The focus of this Section will be on computing these split ratios given known off-ramp flows.

2.4.1 Split Ratios for the Full Access HOT Lane

Consider a node, one of whose output links is an off-ramp, depicted in Figure 2.4. We shall make the following assumptions.

1. Total flow entering the off-ramp, \hat{f}_{222}^{in} , at any given time is known (from measurements) and is not restricted by the off-ramp supply: $\hat{f}_{222}^{in} < R_{222}$.

¹⁰Typical minimum vehicle occupancy level for HOT lanes in the U.S. is 2 (2+HOV) or sometimes 3 (3+HOV).

2. Portions of traffic sent to the off-ramp from the HOT lane and from the GP lane at any given time are equal: $\beta_{1,222}^c = \beta_{11,222}^c = \beta$, $c = 1, \dots, C$.
3. None of the flow coming from the on-ramp (link 111), if such flow exists, is directed toward the off-ramp. In other words, $\beta_{111,222}^c = 0$, $c = 1, \dots, C$.
4. Distribution of flow portions not directed to the off-ramp between the HOT and the GP output links is known. This can be written as: $\beta_{ij}^c = (1 - \beta)\delta_{ij}^c$, where $\delta_{ij}^c \in [0, 1]$, as well as $\beta_{111,j}$, $i = 1, 11$, $j = 2, 22$, $c = 1, \dots, C$, are known.
5. Demand S_i^c , $i = 1, 11, 111$, $c = 1, \dots, C$, and supply R_j , $j = 2, 22$, are given.

At any given time, β is unknown and is to be found.

If β were known, the node model described in [5] (Section 2.1.1) would compute the input-output flows, in particular, $f_{i,222} = \sum_{c=1}^C f_{i,222}^c$, $i = 1, 11$. Define

$$\psi(\beta) = f_{1,222} + f_{11,222} - \hat{f}_{222}^{in}. \quad (2.4.1)$$

Our goal is to find β from the equation:

$$\psi(\beta) = 0, \quad (2.4.2)$$

such that $\beta \in \left[\frac{\hat{f}_{222}^{in}}{S_1 + S_{11}}, 1 \right]$, where $S_i = \sum_{c=1}^C S_i^c$. Obviously, if $S_1 + S_{11} < \hat{f}_{222}^{in}$, the solution does not exist, and the best we can do in this case, is to set $\beta = 1$ directing all traffic from links 1 and 11 to the off-ramp.

Suppose now that $S_1 + S_{11} \geq \hat{f}_{222}^{in}$. For any given \hat{f}_{222}^{in} , $\psi(\beta)$ is a monotonically increasing function of β . Moreover, $\psi\left(\frac{\hat{f}_{222}^{in}}{S_1 + S_{11}}\right) \leq 0$, while $\psi(1) \geq 0$. Thus, the solution of (2.4.2) within given interval exists and can be obtained using the *bisection method*.

The algorithm for finding β follows.

1. Initialize:

$$\begin{aligned}\underline{b}(0) &:= \frac{\hat{f}_{222}^{in}}{S_1 + S_{11}}; \\ \bar{b}(0) &:= 1; \\ k &:= 0.\end{aligned}$$

2. If $S_1 + S_{11} \leq \hat{f}_{222}^{in}$, then set $\beta = 1$ and stop.

3. Run the node model from [5] (Section 2.1.1) with $\beta = \underline{b}(0)$ and evaluate $\psi(\beta)$. If $\psi(\underline{b}(0)) \geq 0$, then set $\beta = \underline{b}(0)$ and stop.

4. Run the node model from [5] (Section 2.1.1) with $\beta = \frac{\underline{b}(k) + \bar{b}(k)}{2}$ and evaluate $\psi(\beta)$. If $\psi\left(\frac{\underline{b}(k) + \bar{b}(k)}{2}\right) = 0$, then set $\beta = \frac{\underline{b}(k) + \bar{b}(k)}{2}$ and stop.

5. If $\psi\left(\frac{\underline{b}(k) + \bar{b}(k)}{2}\right) < 0$, then update:

$$\begin{aligned}\underline{b}(k+1) &= \frac{\underline{b}(k) + \bar{b}(k)}{2}; \\ \bar{b}(k+1) &= \bar{b}(k).\end{aligned}$$

Else, update:

$$\begin{aligned}\underline{b}(k+1) &= \underline{b}(k); \\ \bar{b}(k+1) &= \frac{\underline{b}(k) + \bar{b}(k)}{2}.\end{aligned}$$

6. Set $k := k + 1$ and return to step 4.

2.4.2 Split Ratios for the Separated HOT Lane

The configuration of a node with an off-ramp as one of the output links is simpler in the case of a separated HOT lane, as shown in Figure 2.7. Here, traffic cannot directly go from the HOT lane

to link 222, and, thus, we have to deal only with the 2-input-2-output node. There is a caveat, however. Recall from Section 2.2.2 that in the separate HOT lane case we have destination-based traffic commodities, and split ratios for destination-based traffic are fixed.

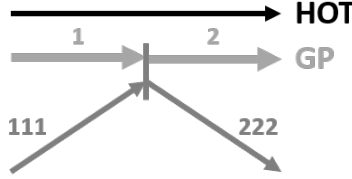


Figure 2.7: A node with a GP link and an on-ramp as inputs, and a GP link and an off-ramp as outputs.

We shall make the following assumptions:

1. Total flow entering the off-ramp, \hat{f}_{222}^{in} , at any given time is known (from measurements) and is not restricted by the off-ramp supply: $\hat{f}_{222}^{in} < R_{222}$.
2. All the flow coming from the on-ramp (link 111), if such flow exists, is directed toward the GP link 2. In other words, $\beta_{111,2}^c = 1$ and $\beta_{111,222}^c = 0$, $c = 1, \dots, C$.
3. Demand S_i^c , $i = 1, 111$, $c = 1, \dots, C$, and supply R_2 are given.
4. Denote the set of destination-based commodities as \mathcal{D} . Split ratios β_{1j}^c for $c \in \mathcal{D}$ are known. Split ratios $\beta_{1j}^c = \beta$ for $c \in \overline{\mathcal{D}}$, where β is to be determined.

The first three assumptions here reproduce assumptions 1, 3 and 5 made for the full access HOT lane case. Assumption 4 is a reminder that there is a portion of traffic flow that we cannot direct to or away from the off-ramp, but we have to account for it.

Similarly to the full access HOT case, define function $\psi(\beta)$:

$$\psi(\beta) = \sum_{c \in \overline{\mathcal{D}}} f_{1,222}^c + \sum_{c \in \mathcal{D}} f_{1,222}^c - \hat{f}_{222}^{in}, \quad (2.4.3)$$

where $f_{1,222}^c$, $c = 1, \dots, C$ are determined by the node model from [5] (Section 2.1.1). The first term of the right-hand side of (2.4.3) depends on β . As before, $\psi(\beta)$ is a monotonically increasing

function. We look for the solution of equation (2.4.2) on the interval $[0, 1]$. This solution exists iff $\psi(0) \leq 0$ and $\psi(1) \geq 0$. The algorithm for finding β is the same as the one presented in the previous section, except that $\underline{b}(0)$ should be initialized to 0, and S_{11} is assumed to be 0.

2.4.3 Summary of the Calibration Process

The model calibration follows the workflow diagram shown in Figure 2.8.

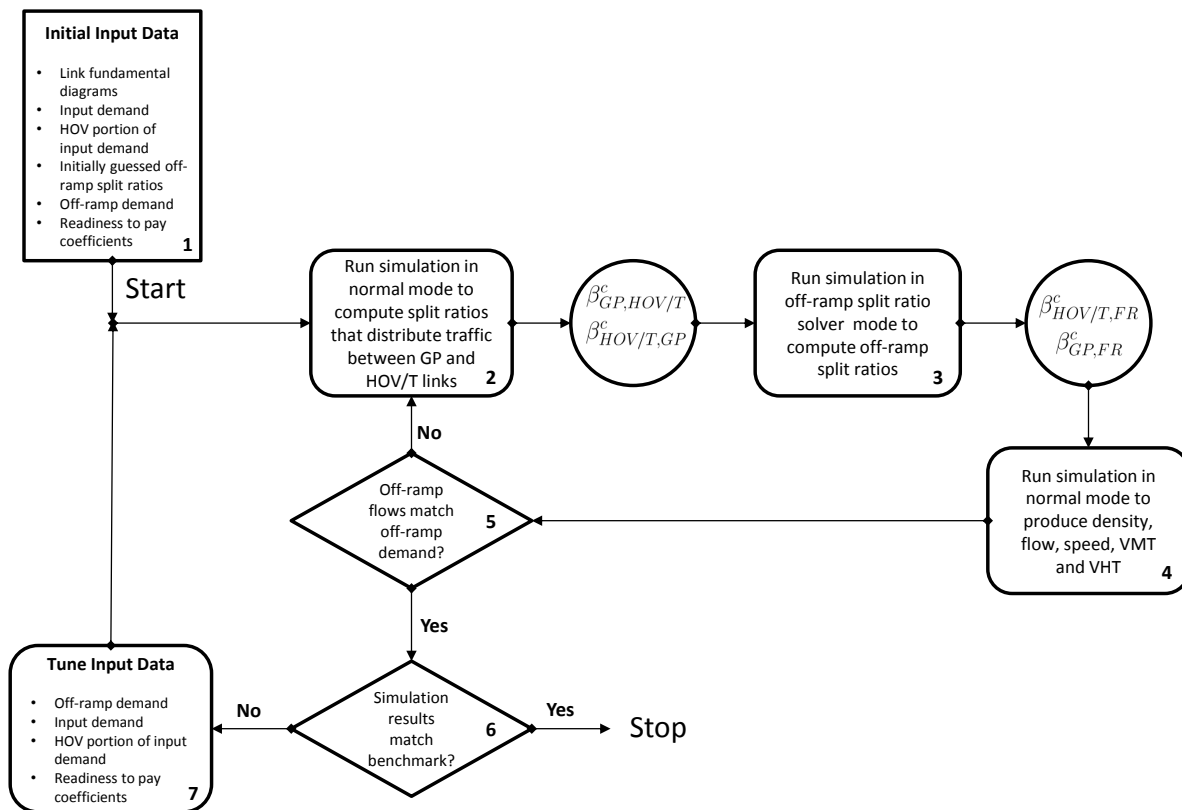


Figure 2.8: Calibration workflow.

1. We start by assembling the available measurement data. Fundamental diagrams are assumed to be given. Mainline and on-ramp demand is specified per 5-minute periods together with the HOV portion parameter indicating the fraction of the input demand that is HOV. Initially we do not know off-ramp split ratios as they cannot be measured directly. So we use some

arbitrary values to represent them and call it “initially guessed off-ramp split ratios”. What can be measured instead of off-ramp split ratios, are the flows directed to off-ramps, to which we refer to as *off-ramp demand*. Finally, if we model the HOT lane, we need the readiness to pay coefficients $\alpha_0, \alpha_1, \alpha_2$ for equation (2.2.10), as well as the probability of the violators being caught. These parameters are obtained as described in Section 2.3.

2. We run the traffic model as described in Section 2.1, where in step 5 the a priori undefined split ratios between traffic in the GP and in the HOT lanes (see expressions (2.2.1)) will be assigned.
3. Using these newly assigned split ratios we run the traffic model again, only this time, instead of using given off-ramp split ratios, we compute them from the given off-ramp demand as described in Sections 2.4.1 and 2.4.2. As a result of this step, we obtain new off-ramp split ratios.
4. Now we run the traffic model as we did originally, in step 2, only this time with new off-ramp split ratios, and record the simulation results — density, flow, speed, as well as performance measures such as vehicle miles traveled (VMT) and vehicle hours traveled (VHT).
5. Check if the resulting off-ramp flows match the off-ramp demand. If yes, proceed to step 6, otherwise, repeat steps 2-5. Usually, it takes the process described in steps 2-5 no more than two iterations to converge.
6. Evaluate the simulation results:
 - correctness of bottleneck locations and activation times;
 - correctness of congestion extension at each bottleneck;
 - correctness of VMT and VHT.

If the simulation results are satisfactory, stop. Otherwise, proceed to step 7.

7. Tune input data in the order shown in block 7 of Figure 2.8.

Chapter 3

I-10 West: Data Analysis and Simulation

3.1 Overview

To evaluate the proposed HOT lane model, we use data from the separated HOT lane with control access on I-10 West freeway in Los Angeles County [8], a 11-mile freeway with 1 ingress-only, 3 egress-only and 2 ingress/egress gates,¹ shown in Figure 3.1.

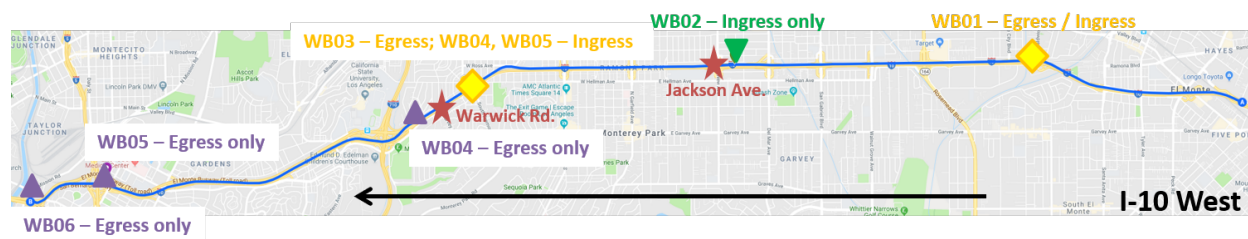


Figure 3.1: Map of the 12-mile I-10 West freeway segment with the HOT lane

Here, WB01, WB02, WB03, WB04, WB05 and WB06 indicate HOT gates. Gates WB01 and WB03 are ingress/egress, gate WB02 is ingress-only, and gates WB04, WB05, WB06 are egress-only. The GP lane has 4 and the HOT lane has 2 sublanes. The HOT lane is always active, but it has two regimes corresponding to peak hours — from 5 to 9 am and from 4 to 7 pm on weekdays; and to

¹Ingress-only gate allows vehicles only to enter the HOT lane. Typically, ingress-only gates are at on-ramps that are directly connected to the HOT lane. Egress-only gate allows vehicles only to exit the HOT lane. Typically, egress-only gates are at off-ramps, to which the HOT lane is connected directly. Ingress/egress gate is a stretch of freeway, where traffic can switch between the GP and HOT lane.

off-peak hours — the rest of the time. During off-peak hours, 2+HOV (vehicles with two riders or more) can use the HOT lane free of charge, and single-occupancy vehicles (SOVs) can use the HOT lane at the fixed price of 25 cents per mile. During peak hours, 3+HOVs (vehicles with three riders or more) can use the HOT lane free of charge, whereas the others are considered LOVs and to use the HOT lane have to pay the toll that varies between 35 and 200 cents per mile depending on the demand for the HOT lane.

We base our analysis on the HOT lane data for the 18-month period starting in December 2015 and ending in May 2017, obtained from LA Metro [8]. These data contain:

- Timestamped FasTrak transponder entry and exit gates, vehicle occupancy indicated by the transponder setting (3+HOV, 2+HOV or SOV) and the toll amount paid.
- Monthly HOT lane FasTrak violations. These are not be confused with HOT lane violations. FasTrak violations refer to those cases when a vehicle registered in the FasTrak system uses a HOT lane without functional FasTrak transponder or its FasTrak account balance does not allow the vehicle to pay the required toll. These kind of violations are registered and the fines issued automatically by the FasTrak system. The fine for the first-time FasTrak violator amounts to \$25. Subsequent violations result in greater charges. Since we do not have the breakdown between first-time and other FasTrak violations, however, we assume a \$25 charge per FasTrak violation.
- Monthly CHP citations. These refer to HOT lane violators being caught. There can be type I and type II HOT lane violations. Type I violation is a crossing of the solid white line separating GP and HOT lanes in the absence of a concrete divider.² Type II violation is the misrepresentation of the LOV as HOV in the HOT to avoid paying the toll. This is done by setting FasTrak transponder to 3+HOV in a car with fewer than three people inside. The minimum fine type I and II violations is \$491. This amount must be paid by first-time violators being caught. Subsequent violations are punished with greater fines. As with FasTrak violations, we do not have a brekdown between first-time and other HOT lane violations. So, we assume a \$491 fine per CHP citation.

²Type I violations happen only on separated HOT lanes with control access, such as I-10 West.

Figure 3.2 presents the statistics of monthly VMT on the studied 11-mile segment of I-10 West, and Figure 3.3 shows the percentage composition of this monthly VMT. Both figures show numbers of total VMT and VMT aggregated only over peak hours.



Figure 3.2: Monthly VMT statistics on I-10 West.

From here we learn that:

- I-10 West HOT lane serves only 10-12% of the total monthly VMT, although it constitutes 1/3 of the free way (2 lanes out of 4), which points to its underutilization.
- We expect, however, that VMT portion served by the HOT lane during peak hours is higher: roughly, 16-20%. This comes from the fact that peak hour HOT lane VMT constitutes roughly 40% of total HOT lane VMT, whereas peak hours take up only 24% of total time.
- 40% of HOT lane VMT is claimed by self-declared 3+HOVs. This portion grows to 50%

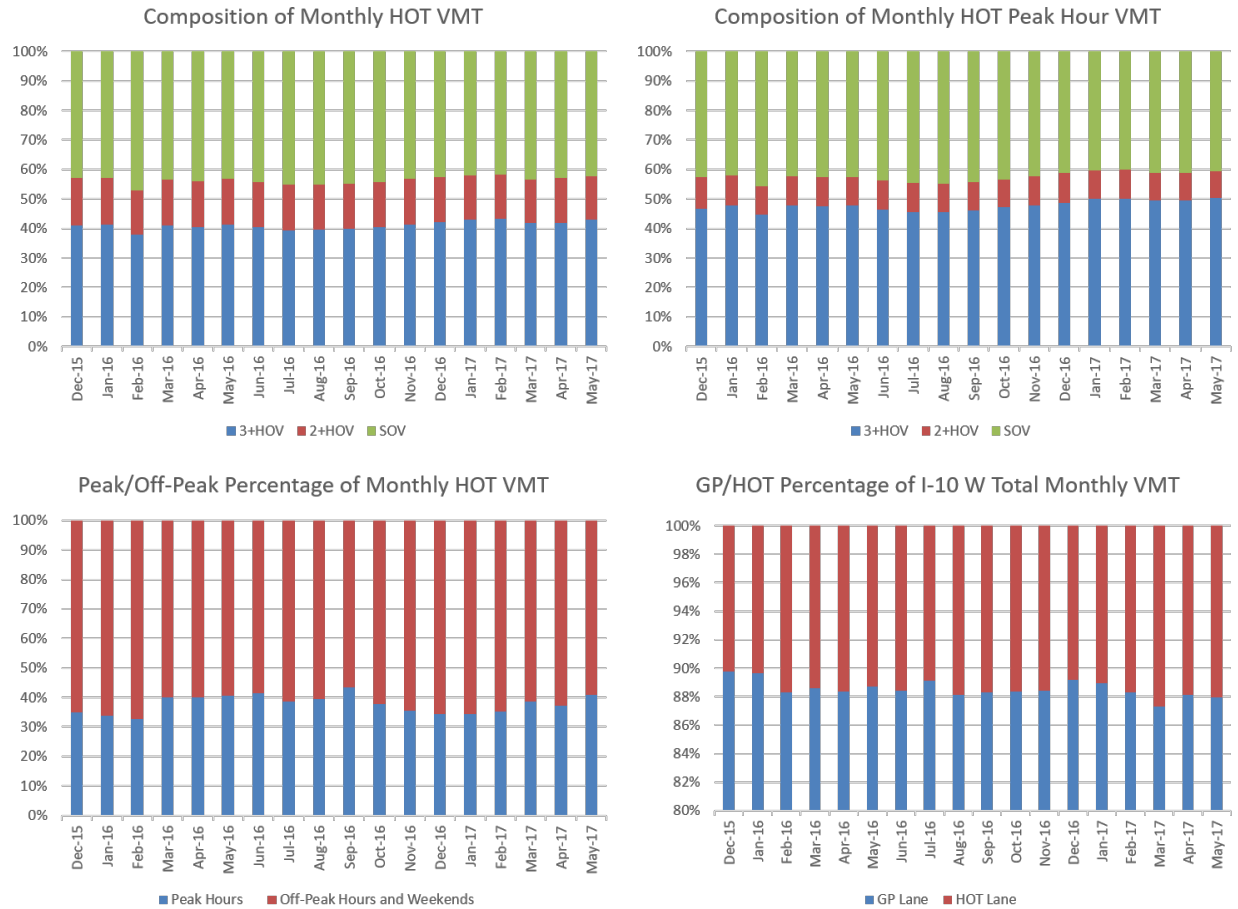


Figure 3.3: Percentage composition of monthly VMT statistics on I-10 West.

during peak hours.

- The self-declared SOV portion of VMT stays almost constant, about 40%.

Figure 3.4 presents the monthly revenue collected from I-10 West HOT lane. Average toll per mile is obtained by dividing monthly peak hour revenue by monthly peak hour HOT lane VMT contributed by LOVs, namely, SOVs and 2+HOVs.

From here we learn that:

- At least 20%, and up to 40% of the HOT lane revenue comes from FasTrak violation fines.
- Up to 70% of HOT operations revenue comes from peak hours.

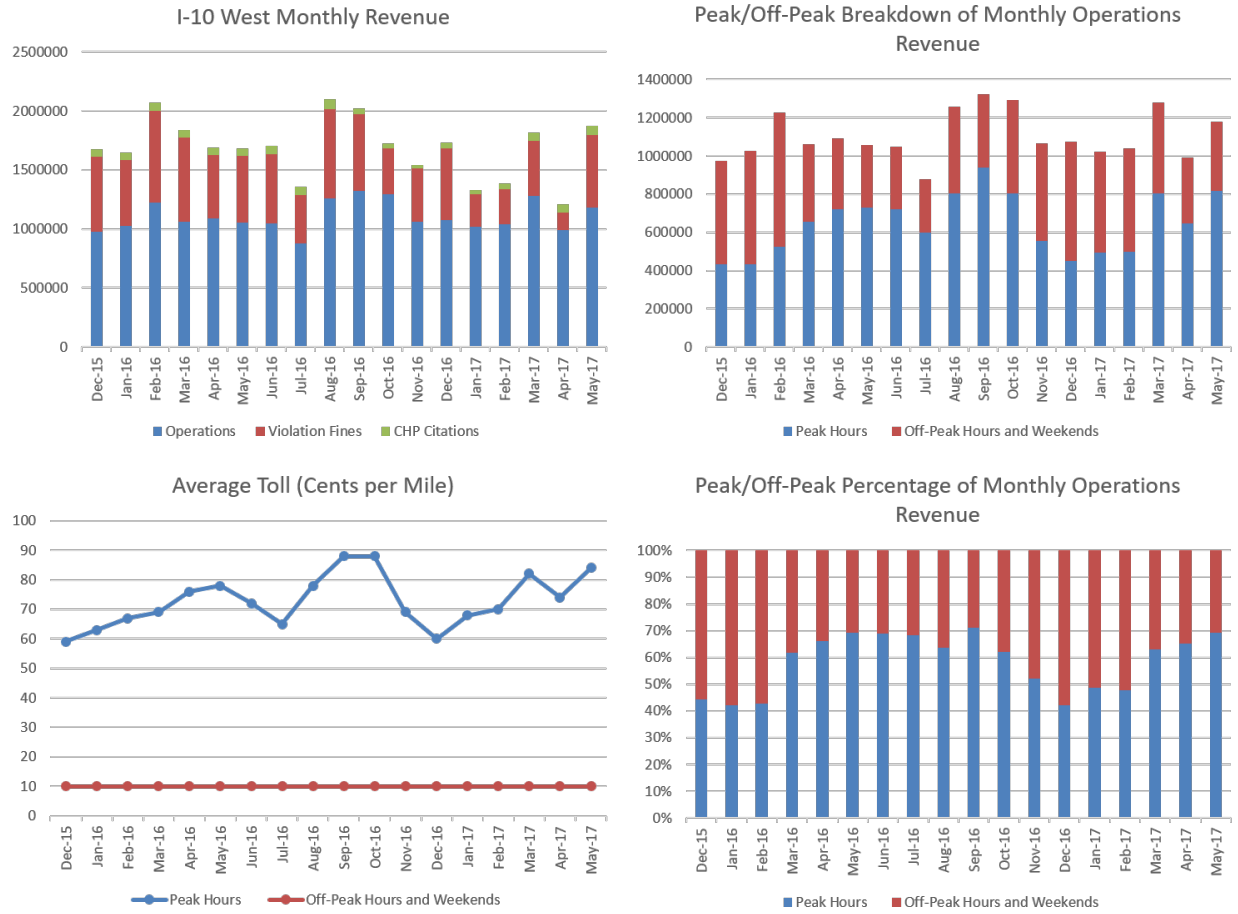


Figure 3.4: Monthly toll and revenue statistics on I-10 West.

- For an average user, HOT lane toll is a monotonic non-decreasing function.³ Non-monotonic nature of the average toll curve indicates the volatility of revenue-to-VMT ratio.

Table 3.1 summarizes the user satisfaction survey conducted by LA Metro in 2017 about I-10 and I-110 HOT facilities.

	Very dissatisfied	Somewhat dissatisfied	Somewhat satisfied	Very satisfied
Time saved vs. toll paid	5.48%	17.9%	37.44%	39.18%
Speed in HOT lane	4.62%	17.21%	40.61%	37.56%
	Strongly disagree	Somewhat disagree	Somewhat agree	Strongly agree
Toll money is worth it	8.92%	24.67%	33.33%	33.07%

Table 3.1: 2017 satisfaction survey for express lanes on I-10 and I-110 taken by LA Metro.

³Toll values only go up, never down. On I-10, maximum toll value went from \$1.40 per mile in 2014 to \$2 in 2016 and is increased to \$2.10 in May 2019.

Next, we discuss the analysis of HOT lane violation data.

3.2 Violation Data Analysis

FasTrak data provide us with an insight about type I violations. Vehicles on I-10 West can legally use only ingress gates to enter and only egress gates to exit the HOT facility. Thus, vehicles that entered the HOT lane through WB01 or WB02 gates cannot have WB01 and WB02 as their exit gates; and vehicles with a WB03, WB04, WB05 or WB06 exit gates cannot have WB03 as an entry gate — see Figure 3.1. All records with exit gates WB01 or WB02, and all records with entry gate WB03 indicate vehicles that crossed between the GP and the HOT lanes over the solid white line. These are type I violators.

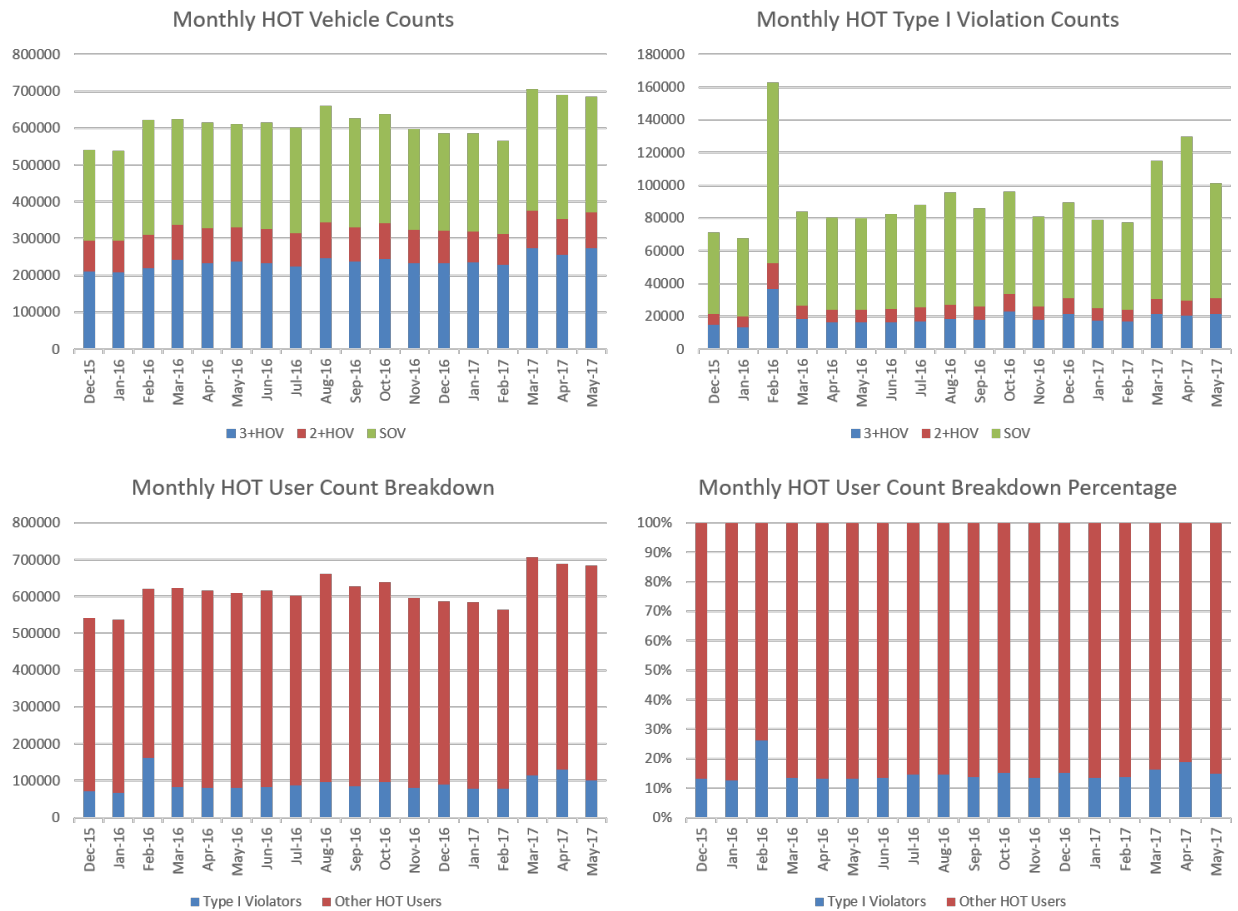


Figure 3.5: I-10 West HOT lane vehicle counts and counts of type I violations.



Figure 3.6: I-10 West HOT lane vehicle counts and counts of type I violations during peak hours.

Figure 3.5 presents the monthly statistics of HOT lane user counts and counts of type I violations. Figure 3.6 shows similar statistics just for peak hours. Figure 3.7 breaks down type I violations into peak and off-peak hours.

From here we learn that:

- About 15% of HOT lane users are type I violators. This number must be treated as a lower bound for type I violations, since these are only those violations registered by FasTrak readers. Other situations, when vehicles cross back and forth between the GP and the HOT lanes outside of FasTrak reader communication zone are left unaccounted for.
- Portion of registered type I violations during peak hours is 10%, which is less than 15% type I violators overall. This is an indicator that the most of these violations are conducted not

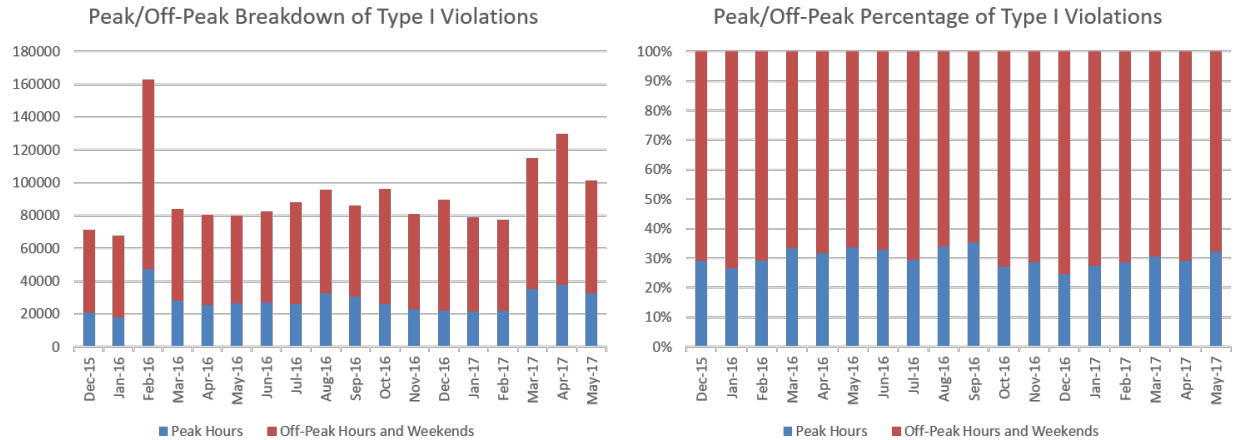


Figure 3.7: Peak/off-peak breakdown of I-10 West HOT lane type I violation counts.

with an intention to cheat the system, but because of impatience or some miscalculation: e.g., HOT lane travelers realizing the need to take certain exit accessible only from the GP lane.

- Most registered type I violators are SOVs — over 70%.
- Most registered type I violations occur during off-peak hours — 70%.

Discussing Figures 3.2 and Figure 3.3, we saw that 40% of HOT lane VMT is claimed by self-declared 3+HOVs, and during peak hours 3+HOV portion of traffic in the HOT lane grows to 50%. Now, the question is: what is the portion of type II violators in the HOV component of the HOT lane traffic?

To obtain some ground truth, Caltrans District 7 ordered the corresponding data collection conducted via manual counts. Data were collected on Tuesdays, October 11 and 18, 2016, between 6.30 and 8.30am at two locations. On October 11 vehicle counts were collected near Warwick Road and on October 18 — near Jackson Avenue. These locations are marked with a star in the I-10 West corridor map (Figure 3.1). The hourly manual counts for the period between 7.00 and 8.00 am are juxtaposed with the FasTrak data in Figure 3.8.

In both cases we see a significant undercount of SOVs and 2+HOVs by the FasTrak system. At the same time, instead of 50% (51%) self-declared 3+HOVs, there are only 16% (9%) of 3+HOV traffic in the HOT lane in the peak hour on October Tuesday. The others are type II violators

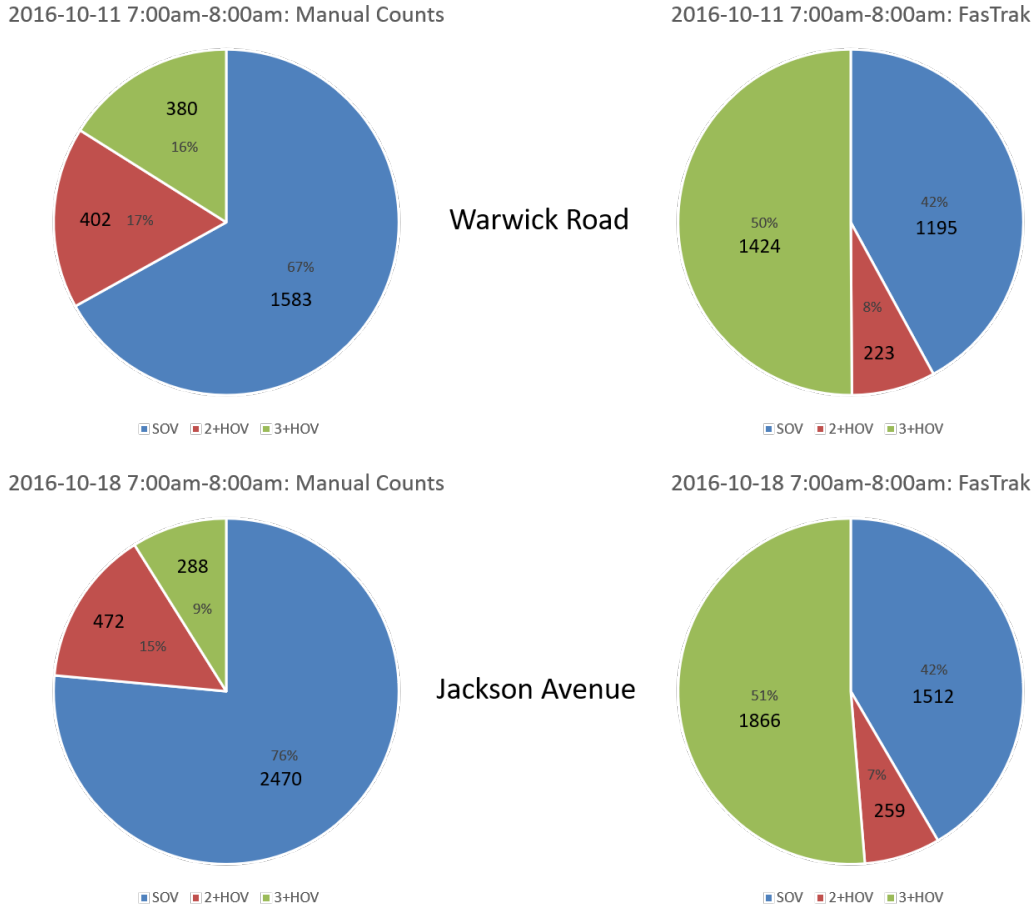


Figure 3.8: Comparison of manual counts with FasTrak data at two measurement points.

misrepresenting themselves as 3+HOVs. Warwick measurements tell us that 84% of HOT lane users must pay, but only 50% do. According to Jackson measurements, 91% of HOT lane users must pay, but only 49% do. We will use must-pay-to-actually-paying ratio 84/50 coming from the Warwick measurement, a less dramatic one, as a reference point.

To assess monthly violation VMT and revenue lost due to type II violations in a systematic way, we compute ratios of peak hour operations revenue to monthly peak hour HOT lane VMT and to the average peak hour toll. The resulting curves are presented in Figure 3.9. Data points marked with a star correspond to October 2016, when manual vehicle counts were collected. Our reference point corresponds to these points on the curves.

The revenue-to-VMT ratio represents the amount of money collected per vehicle-mile in the HOT lane. This curve represents “efficiency” of the collected revenue. The revenue-to-toll ratio represents

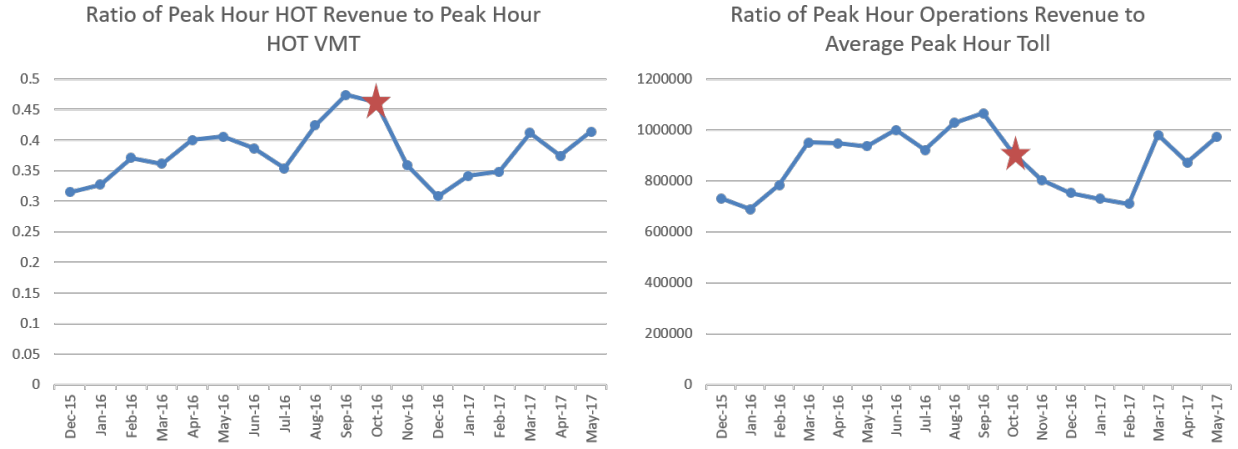


Figure 3.9: Ratios of peak hour monthly operations revenue to monthly peak hour VMT and to average toll. Star indicates the time, when manual counts were collected.

the number of vehicle-miles in the HOTA lane, for which users paid. Points that are higher on the Y-axis in both curves mean a better managed HOTA lane in terms of revenue maximization compared to points that are lower on the Y-axis. We see that the time, when our ground truth about type II violations was collected, is the time of a better HOTA lane management.

We will use the revenue-to-toll curve to compute the adjustment coefficient for month X :

$$\begin{aligned}
 \text{Adjustment Coefficient}(X) &= \\
 \text{Must-Pay-to-Actually-Paying Ratio} &\times \frac{\text{Revenue-to-Toll Ratio(October 2016)}}{\text{Revenue-to-Toll Ratio}(X)} = \\
 \frac{84}{50} &\times \frac{\text{Revenue-to-Toll Ratio(October 2016)}}{\text{Revenue-to-Toll Ratio}(X)}. \tag{3.2.1}
 \end{aligned}$$

Now we can estimate the violation VMT for month X :

$$\begin{aligned}
 \text{Violation VMT}(X) &= \\
 \text{Adjustment Coefficient}(X) &\times \text{LOV VMT}(X) - \text{LOV VMT}(X). \tag{3.2.2}
 \end{aligned}$$

Similarly, the lost revenue for month X is estimated as:

$$\text{Lost Revenue}(X) = \text{Adjustment Coefficient}(X) \times \text{Lost Revenue}(X) - \text{Lost Revenue}(X). \quad (3.2.3)$$

Computed estimates of the violation VMT and the lost revenue are shown in Figure 3.10.

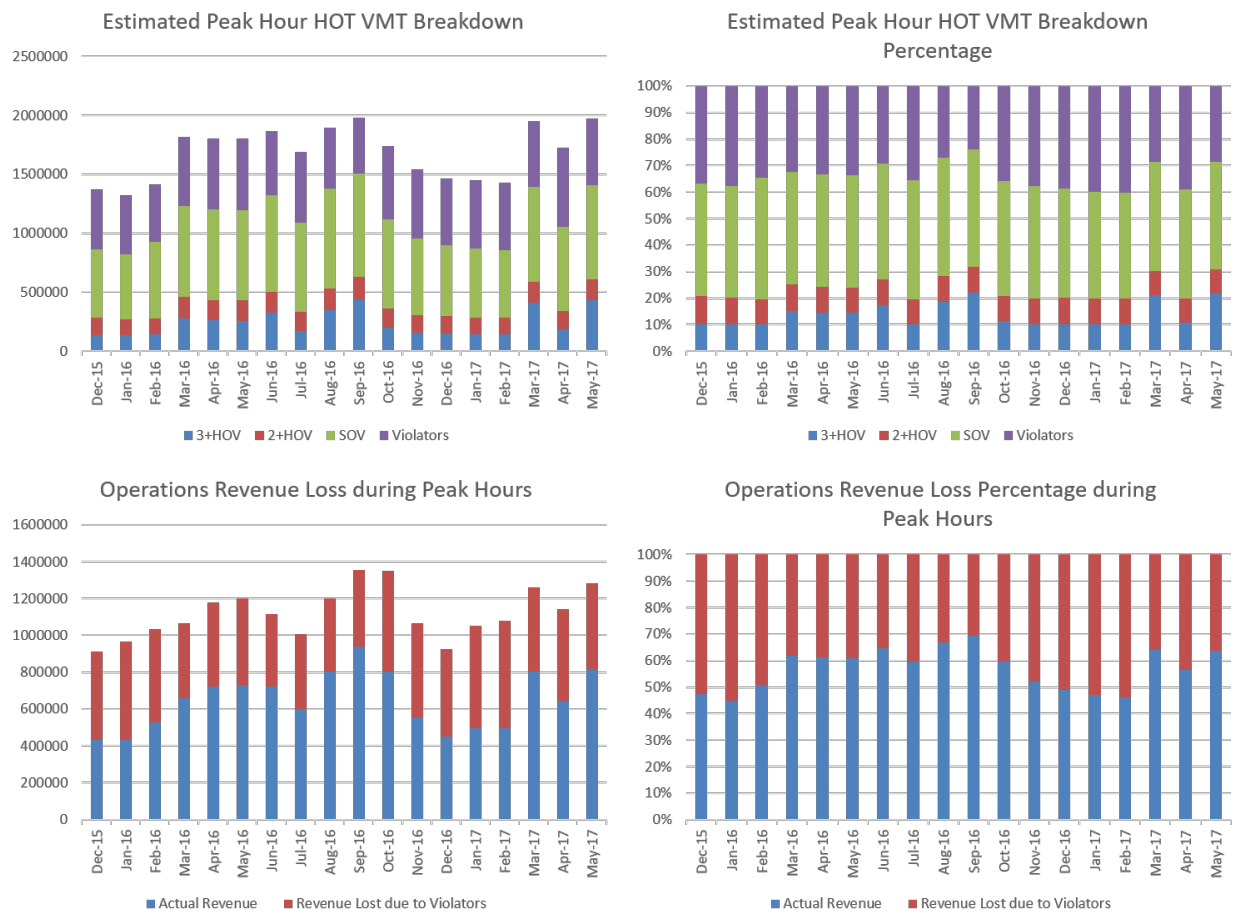


Figure 3.10: Estimated monthly peak hour VMT from violators and revenue loss due to violators.

3.3 Simulation Model

To model the HOT lane, we will consider the road segment around the WB03 gate, shown in Figure 3.11.

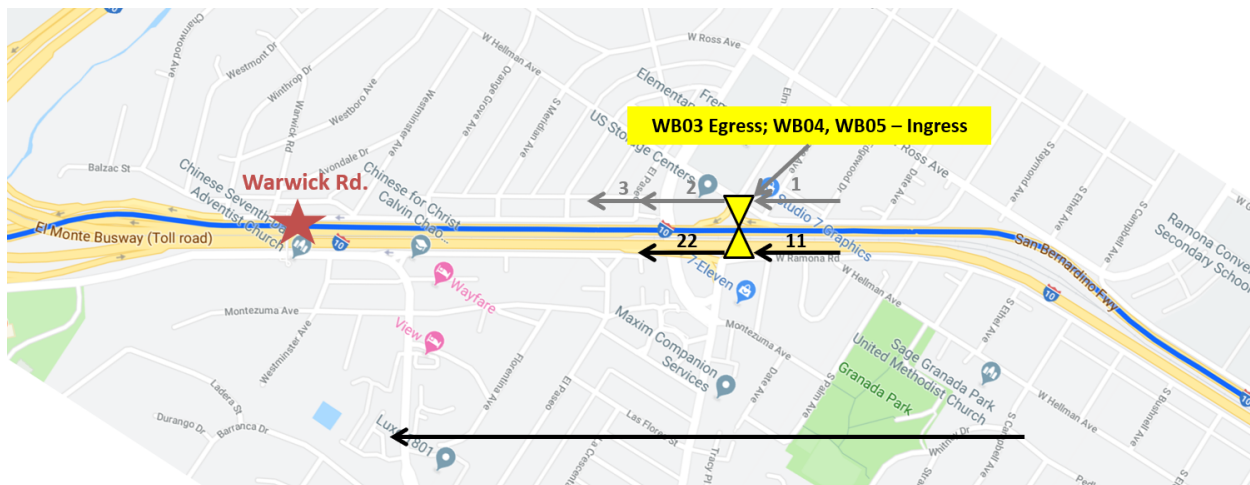


Figure 3.11: Map of the 12-mile I-10 West freeway segment with the HOT lane

Our focus is on the behavior of the HOT controller during peak hours when the HOT lane is dynamically priced between 35 and 200 cents per mile.⁴

We used I-10 West FasTrak data to calibrate and test the HOT controller. We start by building the dependency of the toll value on the vehicle flow in the HOT lane. Figure 3.12 shows this dependency. As we can see, HOT flow varies between 0 and 3,750 vehicles per hour, while the toll value changes in 5-cent increments between 35 and 200 cents per mile. Piecewise linear curve fitting to the data results in the toll lookup table — Table 3.2. Recall from Section 2.2.3 that the toll lookup table is the first part of the HOT controller model. As was mentioned there, this lookup table is typically put together by the operator of the HOT facility. For the purpose of this example, however, we estimated it from the I-10 West toll data.

The second part of the HOT controller, according to Section 2.2.3, is the calculation of the portion of LOV traffic ready to pay for using the HOT lane. We obtain the measurement of readiness to pay $\hat{\rho}^t$ from relation (2.3.1) using the I-10 West toll data that allow us to extract the LOV portion

⁴Starting May 1, 2019, the maximum toll value increased to 210 cents.

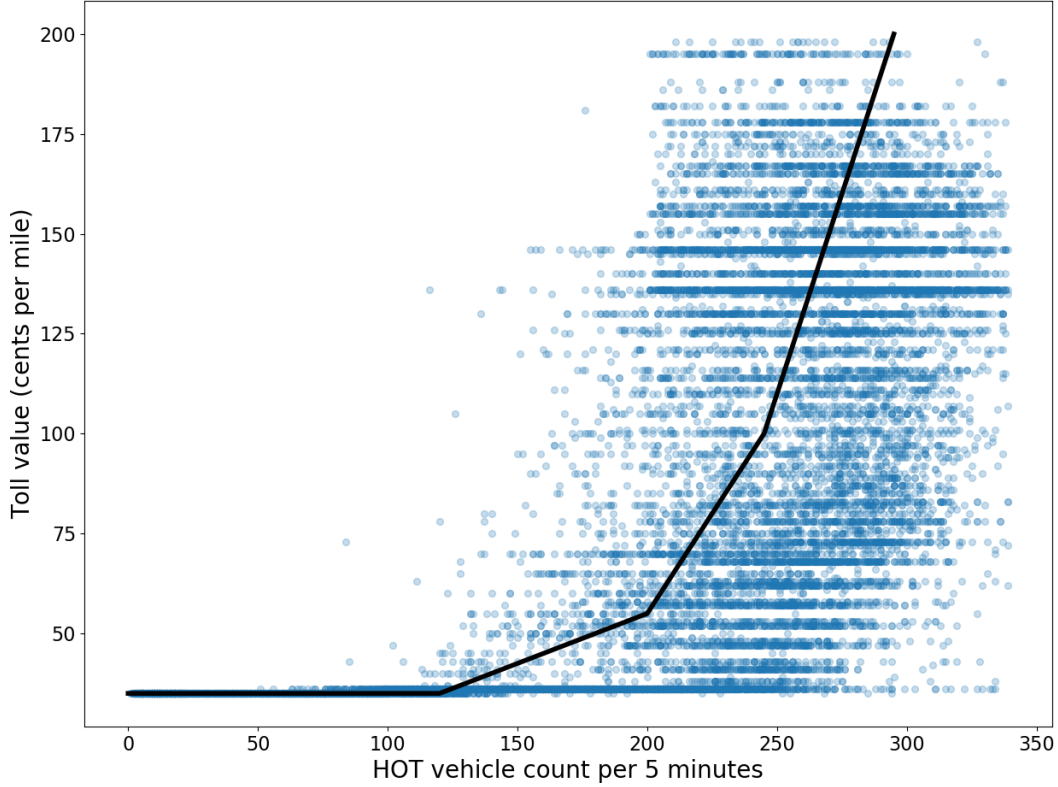


Figure 3.12: Estimation of the toll value based on the flow in the HOT lane.

of the vehicle counts in the HOT lane for the nominator, and PeMS data for the Vehicle Detector Station (VDS) 717073 [2] for the denominator of the right-hand side of (2.3.1).⁵

Figure 3.13 shows the dependency of $\hat{\rho}^t$ on the difference of vehicle densities in the GP and the HOT lanes obtained from the PeMS VDS 717073 (left), and on the toll value (right). We estimate the portion of LOV traffic ready to pay, ρ , according to the expression (2.2.10), as a function of both the GP-HOT density difference and the toll value. Since we have 4 GP and 2 HOT lanes, following (2.3.3),

$$\alpha_0 = \ln(2/4) = -0.6931.$$

⁵We used data for weekdays of October 2016.

From the least squares fit (2.3.5)-(2.3.6), we get

$$\alpha_1 = 0.0115, \quad \alpha_2 = -0.0053.$$

Figure 3.14 shows the surface fitting to the data. The resulting readiness to pay ρ as a function of GP-HOT density difference and toll is shown as a 2-dimensional contour in Figure 3.15.

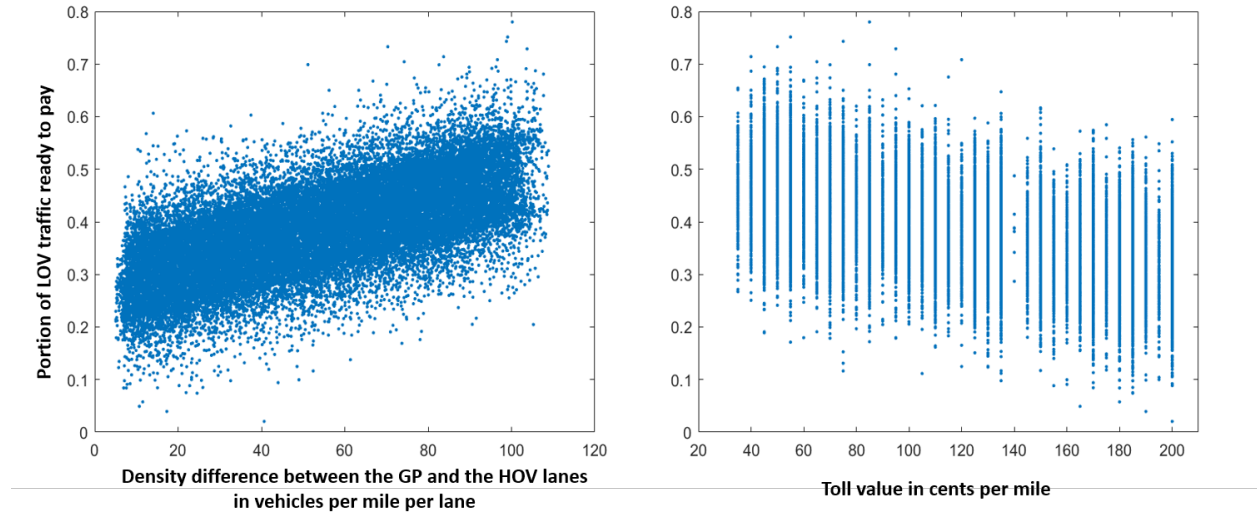


Figure 3.13: Dependency of rediness to pay on difference of traffic density in the GP and the HOV lanes (left); and on the toll value (right).

The choice function $\tilde{\rho}(\cdot)$ for the HOT controller component that computes the portion of LOVs ready to violate depends on the probability of being caught and charged \$491 fine and the present toll value that, multiplied by the remaining travel distance, represents the potential gain.

Using formulae (2.2.13)-(2.2.16) with parameters $\lambda = 1.5$, $\gamma = 0.88$, $\alpha = 0.6$ and $\kappa = 0.01$, we can compute $\tilde{\rho}$ as a function of probability of being caught Pr_2 and the toll value. Figure 3.16 shows this function together with two projections: one with fixed toll 100 cents per mile, the other with fixed probability of being caught 5%.

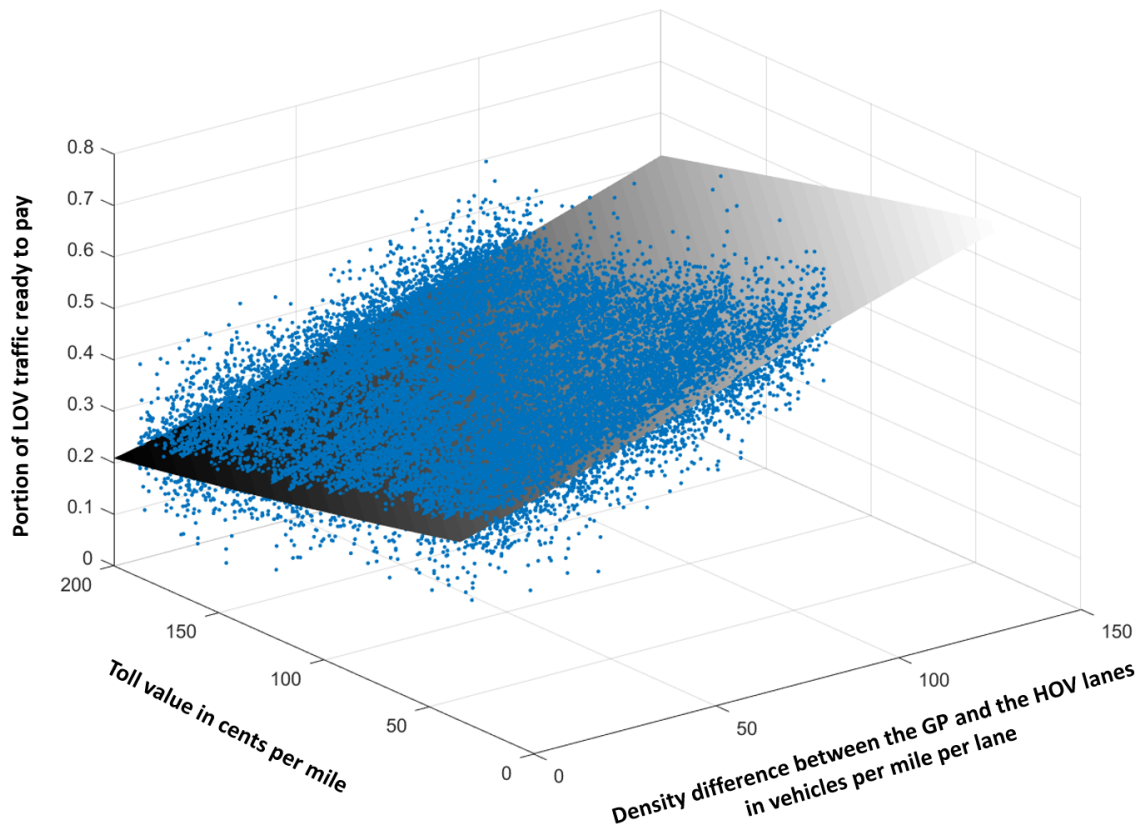


Figure 3.14: Estimation of readiness to pay as a function of density difference between the GP and the HOV lanes and the toll.

HOT lane flow in vehicles per hour	Toll value in cents per mile
0	35.0
1440	35.0
1680	40.0
1920	45.0
2160	50.0
2400	55.0
2460	60.0
2520	65.0
2580	70.0
2640	75.0
2700	80.0
2760	85.0
2820	90.0
2880	95.0
2940	100.0
2970	105.0
3000	110.0
3030	115.0
3060	120.0
3090	125.0
3120	130.0
3150	135.0
3180	140.0
3210	145.0
3240	150.0
3270	155.0
3300	160.0
3330	165.0
3360	170.0
3390	175.0
3420	180.0
3450	185.0
3480	190.0
3510	195.0
3540	200.0

Table 3.2: Toll lookup table.

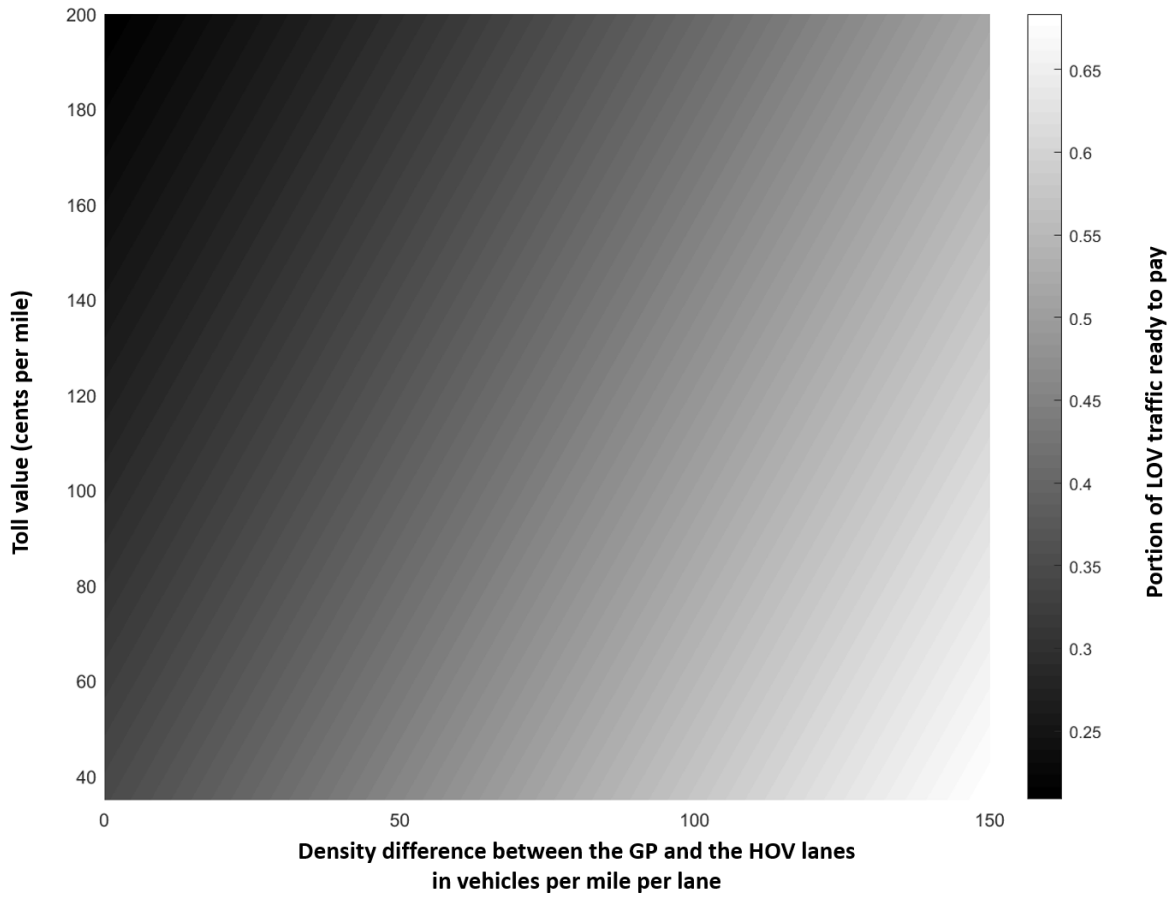
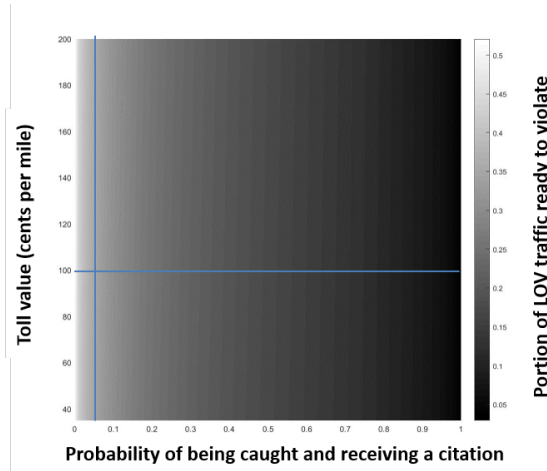
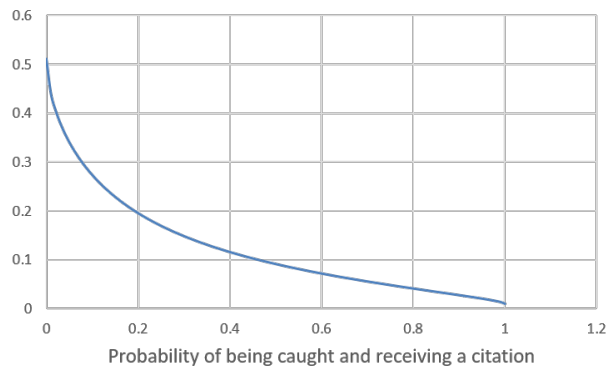


Figure 3.15: Readiness to pay as a function of density difference between the GP and the HOV lanes and the toll.



Portion of LOV Traffic Ready to Violate
(Toll = 100 Cents per Mile)



Portion of LOV Traffic Ready to Violate
(Probability of Being Caught = 5 %)

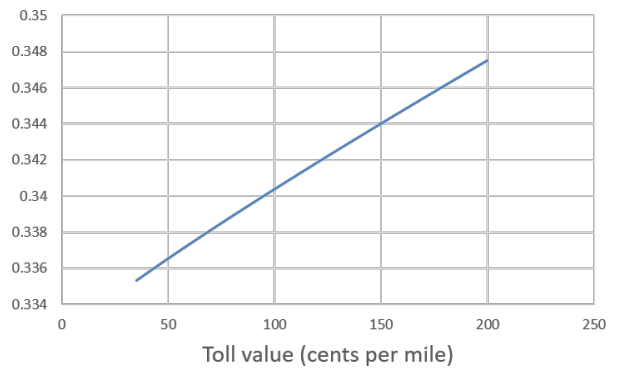


Figure 3.16: Readiness to violate as a function of the probability of being caught and the toll.

Now that the HOT controller is calibrated, we test it in three scenarios.

3.3.1 Scenario 1

Consider the road network configuration as shown in Figure 3.11, where link capacities are:

$$F_1 = 8,000 \text{ vph}, \quad F_2 = 8,000 \text{ vph}, \quad F_3 = 1,600 \text{ vph};$$

$$F_{11} = 3,600 \text{ vph}, \quad F_{22} = 3,600 \text{ vph};$$

$$F_{111} = 2,000 \text{ vph}.$$

Input demand for links 1 and 11 is constant:

$$d_1^1 = 6,700 \text{ vph}, \quad d_1^2 = 0 \text{ vph}, \quad d_1^3 = 0 \text{ vph};$$

$$d_{11}^1 = 0 \text{ vph}, \quad d_{11}^2 = 385 \text{ vph}, \quad d_{11}^3 = 0;$$

$$d_{111}^1 = 85 \text{ vph}, \quad d_{111}^2 = 15 \text{ vph}, \quad d_{111}^3 = 0 \text{ vph}.$$

As we can see, GP link 3 with its low capacity creates a bottleneck for traffic that stays in the GP lane.

Figure 3.17 presents the results of the simulation: LOV and HOV input demand (top-left); flows entering the GP link 2 and the HOT link 22 (bottom-left); toll value (top-right); and the portion of LOV traffic ready to pay the corresponding toll. The system reaches the equilibrium at 80 cents per mile with 37% of LOVs ready to pay.

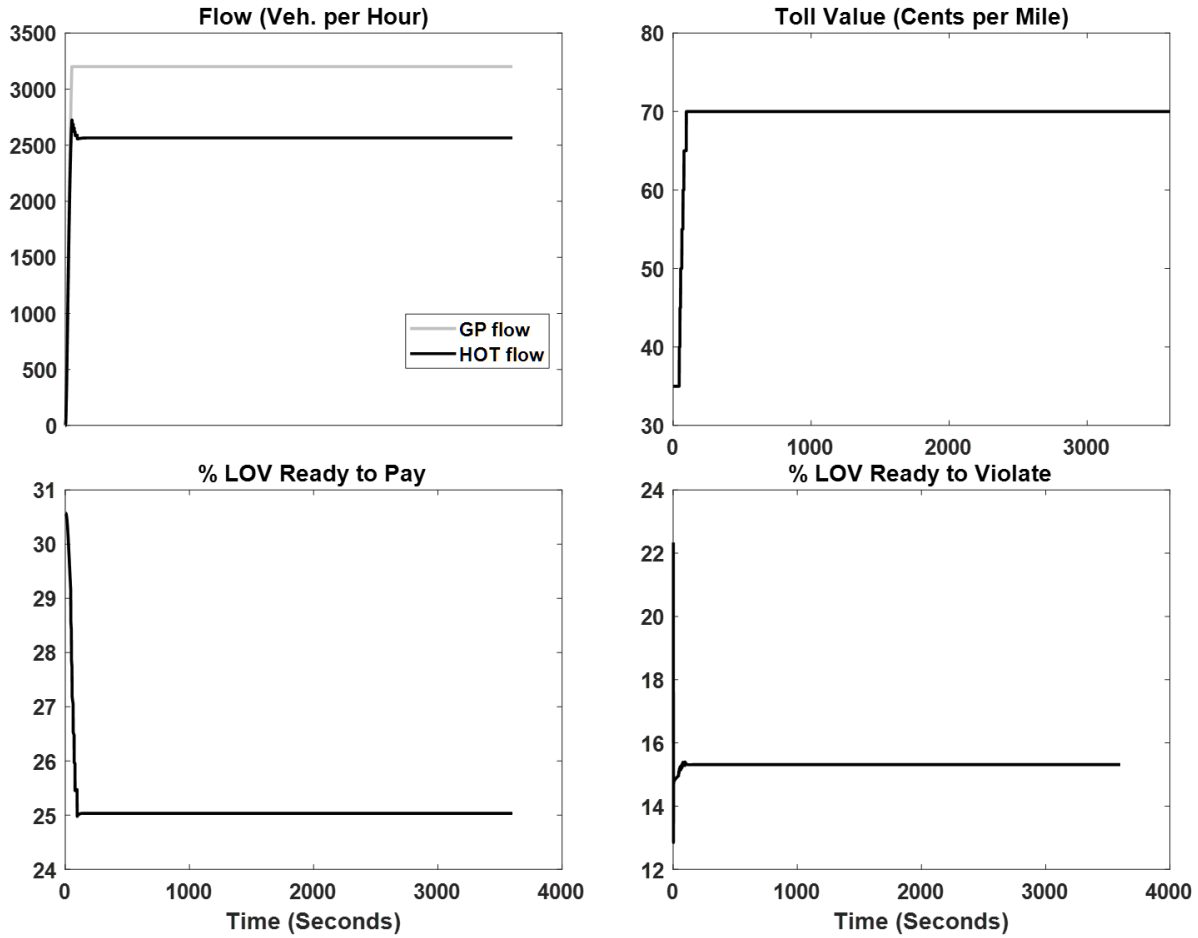


Figure 3.17: Scenario 1 — constant LOV and HOV demand.

3.3.2 Scenario 2

This scenario differs from the scenario 1 only in the HOV demand coming into the HOT lane:

$$d_{11}^2 = 2,585 \text{ vph.}$$

As shown in Figure 3.18, more vehicles enter now the HOT link 22 (bottom-left); the toll value goes up accordingly, to 135 cents per mile; and the readiness to pay drops to 27%.

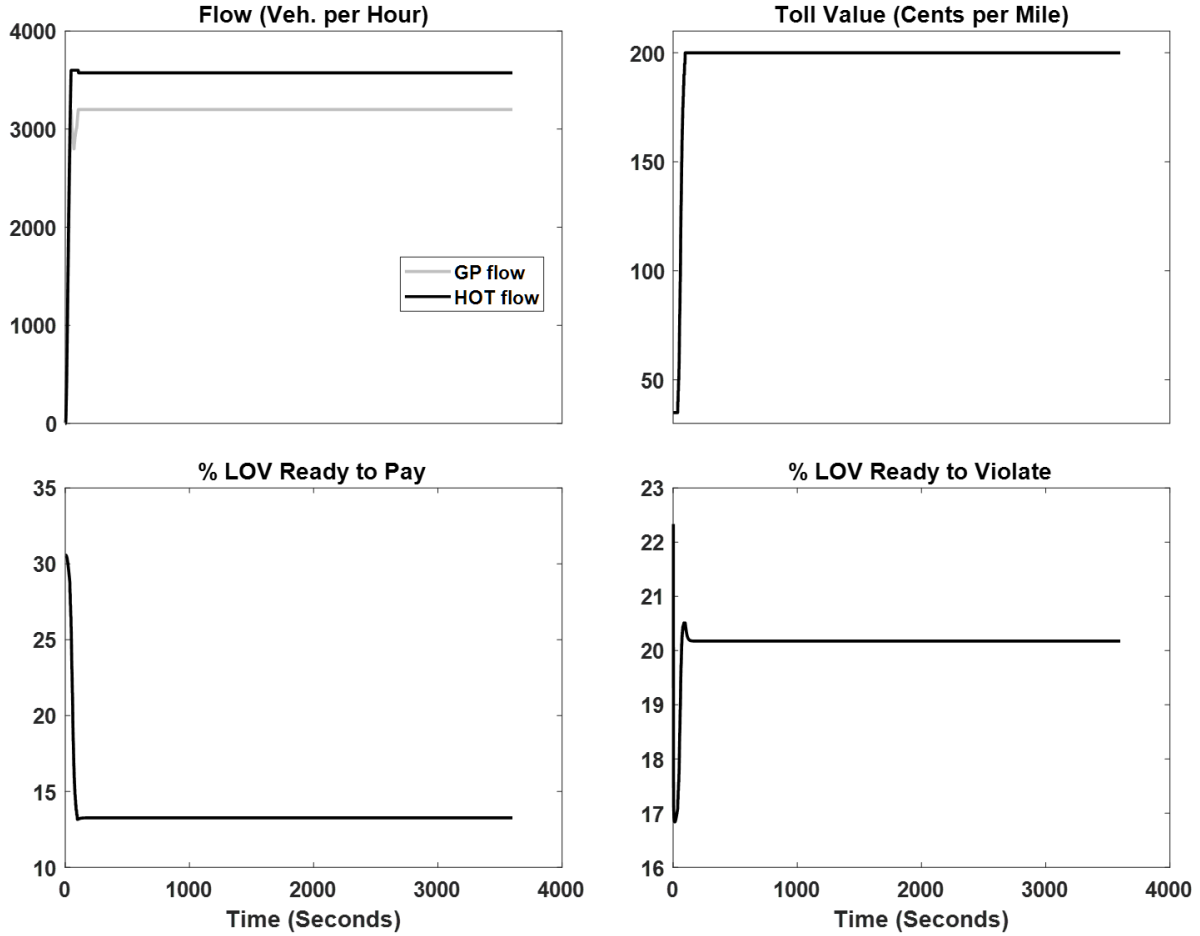


Figure 3.18: Scenario 2 — the same as scenario 1, but has higher HOV demand.

3.3.3 Scenario 3

In this scenario, we set capacity of the GP link 3:

$$F_3 = 7,600 \text{ vph.}$$

The simulation is divided into 4 time periods. The LOV and the HOV demand in links 1 and 11 changes from period to period as specified in Table 3.3.

	Time period 1	Time period 2	Time period 3	Time period 4
d_1^1 (vph)	7,500	7,600	4,000	6,000
d_{11}^2 (vph)	3,500	1,940	2,240	2,440

Table 3.3: Varying demand.

On-ramp demand is constant:

$$d_{111}^1 = 340 \text{ vph}, \quad d_{111}^2 = 60 \text{ vph}.$$

The results of the simulation are shown in Figure 3.19.

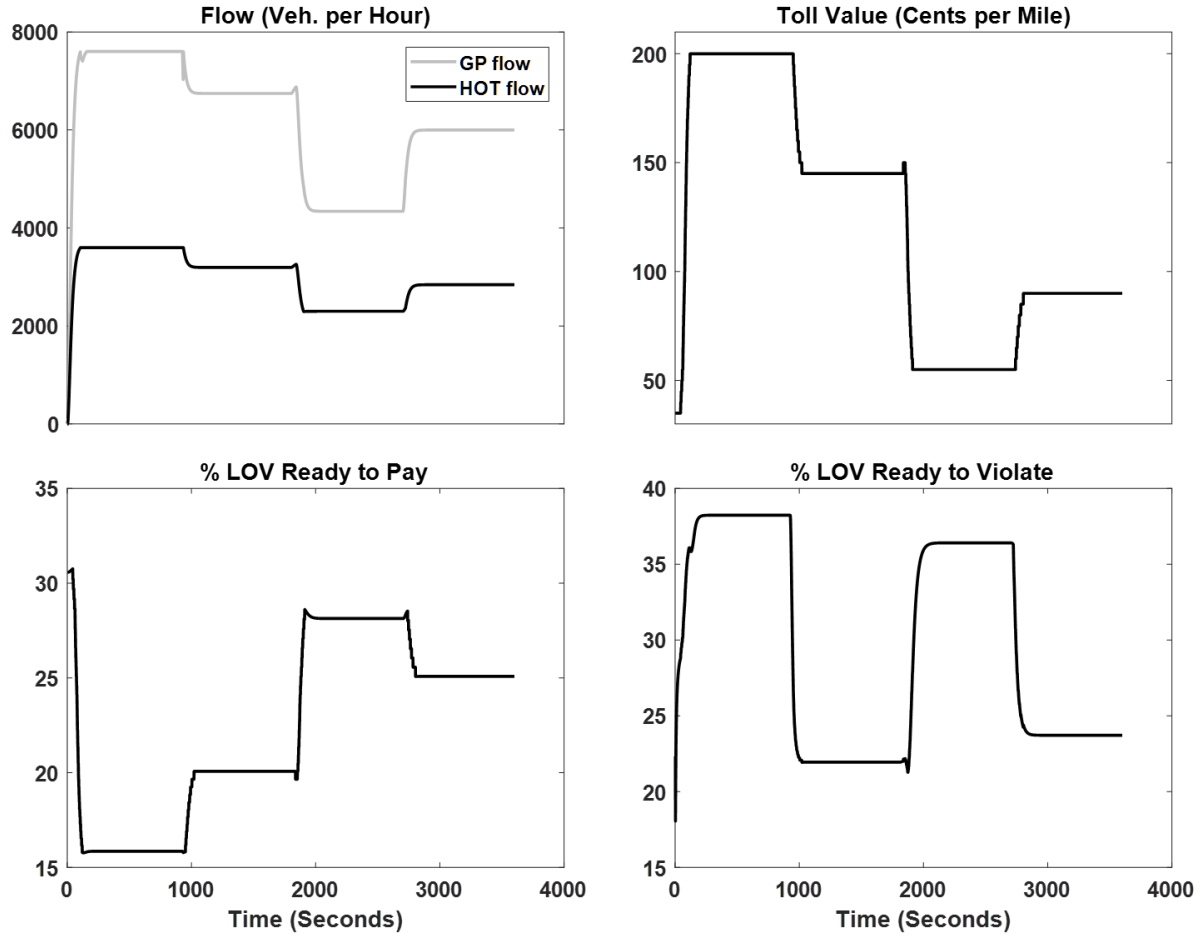


Figure 3.19: Scenario 3 — varying LOV and HOV demand.

Chapter 4

Conclusion

In the course of this project we developed a multimodal macroscopic simulation model for freeway corridors with HOT lanes. This model incorporates the violators' behavior. It was implemented in the Berkeley Advanced Traffic Simulator (BeATS) [1] and tested it with I-10 West HOT data. As test examples show, the model can adequately represent traffic behavior in the presence of multiple vehicle classes and managed lane facilities. We also provided a model calibration methodology. Using I-10 West HOT lane data, we presented the methodology for quantitative assessment of HOT policy violations as well as their impact on HOT facility operation and revenue.

This project is an important contribution to the development of the Operations Planning Toolbox (OPT), a presently ongoing project sponsored by Caltrans. OPT is an open source software toolbox for evaluation of transportation planning and operational scenarios. Incorporating the results of the current project, OPT will have the following capabilities:

- Evaluate operational scenarios of freeway networks with HOV/T facilities;
- Assess impact of various toll strategies accounting for violators' impact;
- Given a traffic pattern, estimate HOT revenue projections and lost revenue due to violations;
- Optimize dynamic toll strategy;
- Optimize ramp metering plans in coordination with HOT lane pricing.

Bibliography

- [1] Berkeley Advanced Traffic Simulator. <https://github.com/ggomes/otm-sim>.
- [2] California Department of Transportation. PeMS homepage. <http://pems.dot.ca.gov>.
- [3] R. Courant, K. Friedrichs, and H. Lewy. Über die partiellen Differenzgleichungen der mathematischen Physik. *Mathematische Annalen*, 100(1):32–74, 1928.
- [4] G. Dervisoglu, G. Gomes, J. Kwon, A. Muralidharan, P. Varaiya, and R. Horowitz. Automatic calibration of the fundamental diagram and empirical observations on capacity. *88th Annual Meeting of the Transportation Research Board, Washington, D.C., USA*, 2009.
- [5] R. Horowitz, A. Kurzhanskiy, A. Siddiqui, and M. Wright. Modeling and control of HOT lanes. Technical Report UCConnect Final, UC Berkeley PATH, 2016. <https://escholarship.org/uc/item/9mx3903c>.
- [6] K. Jang and M. Cassidy. Dual influences on vehicle speed in special-use lanes and critique of US regulation. *Transportation Research, Part A*, 46(2012):1108–1123, 2012.
- [7] D. Kahneman and A. Tversky. Prospect Theory: An Analysis of Decision under Risk. *Econometrica*, 47(2):263–291, 1979.
- [8] Los Angeles County Metropolitan Transportation Authority. Metro Express Lanes. <http://www.metroexpresslanes.net>.
- [9] D. Schmeidler and P. Wakker. Expected Utility and Mathematical Expectation. In *Palgrave Macmillan (eds) The New Palgrave Dictionary of Economics*, London, 1987.

- [10] C. M. J. Tampère, R. Corthout, D. Cattrysse, and L. H. Immers. A generic class of first order node models for dynamic macroscopic simulation of traffic flows. *Transportation Research, Part B*, 45(1):289–309, 2011.
- [11] A. Tversky and D. Kahneman. Advances in Prospect Theory: Cumulative Representations of Uncertainty. *Journal of Risk and Uncertainty*, 5:297–323, 1992.